Global analysis of SUMO chain function reveals multiple roles in chromatin regulation

Tharan Srikumar,[1,2] Megan C. Lewicki,[1,2] Michael Costanzo,[3] Johnny M. Tkach,[3,4] Harm van Bakel,[3,5,] Kyle Tsui,[3,6] Erica S. Johnson,[8] Grant W. Brown,[3,4] Brenda J. Andrews,[3,5,7] Charles Boone,[3,5,7] Guri Giaever,[3,6,7] Corey Nislow,[3,5,7] and Brian Raught[1,2]

[1]Ontario Cancer Institute, University Health Network, Toronto, Ontario M5G 1L7, Canada
[2]Department of Medical Biophysics, [3]Terence Donnelly Center for Cellular and Biomolecular Research, [4]Department of Biochemistry, [5]Banting and Best Department of Medical Research, [6]Department of Pharmaceutical Sciences, and [7]Department of Molecular Genetics, University of Toronto, Toronto, Ontario M5S 1A1, Canada
[8]Department of Biochemistry and Molecular Biology, Thomas Jefferson University, Philadelphia, PA 19107

Like ubiquitin, the small ubiquitin-related modifier (SUMO) proteins can form oligomeric "chains," but the biological functions of these superstructures are not well understood. Here, we created mutant yeast strains unable to synthesize SUMO chains (*smt3*^{allR}) and subjected them to high-content microscopic screening, synthetic genetic array (SGA) analysis, and high-density transcript profiling to perform the first global analysis of SUMO chain function. This comprehensive assessment identified 144 proteins with altered localization or intensity in *smt3*^{allR} cells, 149 synthetic genetic interactions, and 225 mRNA transcripts (primarily consisting of stress- and nutrient-response genes) that displayed a >1.5-fold increase in expression levels. This information-rich resource strongly implicates SUMO chains in the regulation of chromatin. Indeed, using several different approaches, we demonstrate that SUMO chains are required for the maintenance of normal higher-order chromatin structure and transcriptional repression of environmental stress response genes in budding yeast.

Complete image-based screen data

http://jcb-dataviewer.rupress.org/jcb/browse/6156/S52/

Introduction

The small ubiquitin-related modifier (SUMO) system plays important roles in many diverse biological processes in all eukaryotes (Johnson, 2004; Kerscher et al., 2006). Like ubiquitin, SUMO modification is effected via covalent conjugation to an epsilon amine moiety of a lysine residue in a targeted protein, via the sequential action of SUMO-specific E1, E2, and E3 proteins. SUMO conjugation can be reversed by a family of SUMO-specific proteases (Johnson, 2004; Kerscher et al., 2006; Shin et al., 2012).

The sole budding yeast SUMO protein is encoded by the essential *SMT3* gene. Invertebrates also express a single SUMO protein, whereas vertebrates and plants express multiple SUMO isoforms (Hay, 2005; Castro et al., 2012). Systematic proteomics screens have identified >500 putative SUMO conjugates in budding yeast (among others, Wohlschlegel et al., 2004; Denison et al., 2005; Cremona et al., 2012) and hundreds more in plants, insects, and mammals (Nie et al., 2009; Elrouby and Coupland, 2010; Bruderer et al., 2011). Ectopic expression of the human SUMO-1 protein rescues *smt3* lethality (Takahashi et al., 1999), highlighting the usefulness of *Saccharomyces cerevisiae* as a model organism for assessing SUMO function in eukaryotes.

The SUMO proteins interact with small hydrophobic domains referred to as SUMO-interacting motifs (SIMs). SIMs confer low affinity binding to SUMOs, often occur in tandem, and can confer specificity for particular SUMO isoforms (Prudden et al., 2007; Sun et al., 2007; Perry et al., 2008; Tatham et al., 2008). Sumoylation thus represents a rapid and efficient way to regulate protein–protein interactions. SUMO–SIM interactions have been implicated in a variety of biological functions,

Correspondence to Brian Raught: brian.raught@uhnres.utoronto.ca

Abbreviations used in this paper: CUT, cryptic unstable transcript; GO, gene ontology; HCS, high content screen; HU, hydroxyurea; INM, inner nuclear membrane; MMS, methyl methanesulfonate; O/N, overnight; qPCR, quantitative PCR; rDNA, ribosomal DNA; SGA, synthetic genetic array; SIM, SUMO-interacting motif; STUbL, SUMO-targeted ubiquitin ligase; SUMO, small ubiquitin-related modifier; TS, template switch; WT, wild type.

The Rockefeller University Press $30.00
J. Cell Biol. Vol. 201 No. 1 145–163
www.jcb.org/cgi/doi/10.1083/jcb.201210019

including transcriptional control (Ouyang et al., 2009; Santiago et al., 2009; Saether et al., 2011), DNA damage repair (Li et al., 2010; Galanty et al., 2012; Yin et al., 2012), protein degradation (Prudden et al., 2007; Perry et al., 2008), and the assembly of DNA–protein superstructures such as PML (Lallemand-Breitenbach et al., 2008; Tatham et al., 2008) and insulator bodies (MacPherson et al., 2009; Golovnin et al., 2012).

Notably, SUMO can be conjugated to proteins in a monomeric form, or as oligomeric SUMO "chain" structures. In budding yeast, SUMO–SUMO linkages are formed primarily via K15 (Bencsath et al., 2002), although we and others have detected linkages at additional lysine residues in vitro (Bencsath et al., 2002; Jeram et al., 2010). The best characterized function of SUMO chains is as a secondary degradation signal. The SUMO-targeted ubiquitin ligases (STUbLs) are an evolutionarily conserved family of ubiquitin E3 proteins that contain multiple SIMs. The STUbLs are thus recruited to polysumoylated proteins and effect their ubiquitylation, marking them for 26S proteasome-mediated destruction (Perry et al., 2008). A few STUbL targets have been identified, including PML (Lallemand-Breitenbach et al., 2008; Tatham et al., 2008), the HTLV-1 Tax protein (Fryrear et al., 2012), the *Drosophila melanogaster* transcriptional repressor Hairy (Abed et al., 2011), and the budding yeast transcriptional regulator Mot1 (Wang et al., 2006; Wang and Prelich, 2009). Importantly, however, the biological functions of SUMO chains remain poorly characterized.

Many studies have implicated the SUMO system in transcriptional regulation (Garcia-Dominguez and Reyes, 2009; Abed et al., 2011). Transcription factors and coregulators, chromatin remodeling proteins, and histones are all modified by SUMO (Shiio and Eisenman, 2003; Nathan et al., 2006). Most studies have indicated that SUMO plays a negative regulatory role in transcription, and SUMOs can bind to SIMs in transcriptional co-repressors such as CoREST1 (Ouyang et al., 2009) and Daxx, and other types of proteins that regulate chromatin structure, including histone methyltransferases (SETDB1, SUV4-2OH) and the chromatin remodeler Mi2 (Ivanov et al., 2007; Stielow et al., 2008a,b), possibly to effect local heterochromatization (Ross et al., 2002; Yang and Sharrocks, 2004; Ivanov et al., 2007).

Here, using a combination of high-content microscopic screening, functional genomics analysis, and high-density transcript profiling, we conducted the first global study of SUMO chain function. Using this data-rich resource, we implicate the SUMO system in the maintenance of transcriptional repression and higher-order chromatin structure.

Results

smt3^{allR} strains exhibit chromosome segregation defects and replication-associated DNA damage

To better understand the biological roles of SUMO chains, we generated haploid yeast strains in which the endogenous SUMO gene (*SMT3*) was replaced by an ORF in which all nine lysine codons were mutated to code for arginine (as in Bylebyl et al., 2003). The resulting mutant SUMO "allR" polypeptide can thus be conjugated to other proteins as a monomer, but lacks the ability to form SUMO chains (Fig. 1 A). Although *smt3* deletants arrest in G2/M with short spindles and replicated DNA (Seufert et al., 1995; Li and Hochstrasser, 1999; Hochstrasser, 2000), an earlier study demonstrated that *smt3*^{allR} strains are viable and that the SUMO allR polypeptide is conjugated to the septin protein Cdc11 in vivo (Bylebyl et al., 2003). SUMO function is thus at least partially fulfilled by the SUMO allR protein. Consistent with these data, we found that a recombinant SUMO allR protein is conjugated to a model substrate (a biotinylated 11-aa peptide containing the SUMO consensus sequence) in vitro as efficiently as the wild-type (WT) protein (Fig. 1 B), which indicates that the K-to-R mutations do not appreciably affect the ability of this polypeptide to be recognized by the SUMO E1 or E2 proteins.

Several previous studies have demonstrated that steady-state sumoylation increases in response to stress (Zhou et al., 2004; Tempé et al., 2008). To determine whether the *smt3*^{allR} strain is able to respond to environmental stresses commonly encountered by yeast, we assessed its response to high ethanol (EtOH) concentrations. As expected, exposure of WT cells to 10% EtOH (for 1 h) led to a dramatic increase in high-molecular-weight SUMO conjugates (Fig. 1 C). Although *smt3*^{allR} cells displayed a decrease in unconjugated (free) SUMO, only a very minor increase in high-molecular-weight SUMO conjugates in response to EtOH treatment was observed (Fig. 1 C; the minor high molecular signal most likely reflects multi-monosumoylation of high-molecular-weight targets, or could represent, e.g., proteins that are both sumoylated and ubiquitylated in response to stress). In addition, here we tested two different *smt3*^{allR} strains: one in which the C-terminal three amino acid extension of the SUMO protein was maintained in the coding region (pro-*smt3*^{allR}) and a second in which this region was removed to express the mature SUMO polypeptide (*smt3*^{allR}). No differences in division time (not depicted) or EtOH response were observed between the two strain types (Fig. 1 C), which indicates that SUMO maturation activity is not limiting in these cells.

The signal strength of the unconjugated SUMO allR protein in Western blot analysis was markedly lower than that observed for the endogenous WT SUMO protein (Fig. 1 C). However, when equal amounts of purified recombinant WT and allR SUMO polypeptides were subjected to SDS-PAGE and Coomassie blue staining (Fig. 1 D, top) or Western blotting analysis (Fig. 1 D, bottom), we found that the allR SUMO protein is simply not recognized as efficiently by the SUMO antibody (with this antibody, the allR protein yields <20% of the signal intensity of an equivalent amount of the WT SUMO protein). Indeed, quantification of SUMO signal intensity in parental and *smt3*^{allR} yeast strains based on these data indicate that the SUMO allR protein is expressed at levels similar to (or even higher than) the endogenous SUMO protein (see Materials and methods for details).

As expected (Bylebyl et al., 2003), under standard culture conditions the doubling time of *smt3*^{allR} cells is increased ~1.5-fold (180 ± 6.7 min) as compared with parental strains (119 ± 1.3 min; $P < 0.01$; Fig. 2 A). FACS of SYTOX green–stained cells revealed a slight increase in a supra-G2 population, and

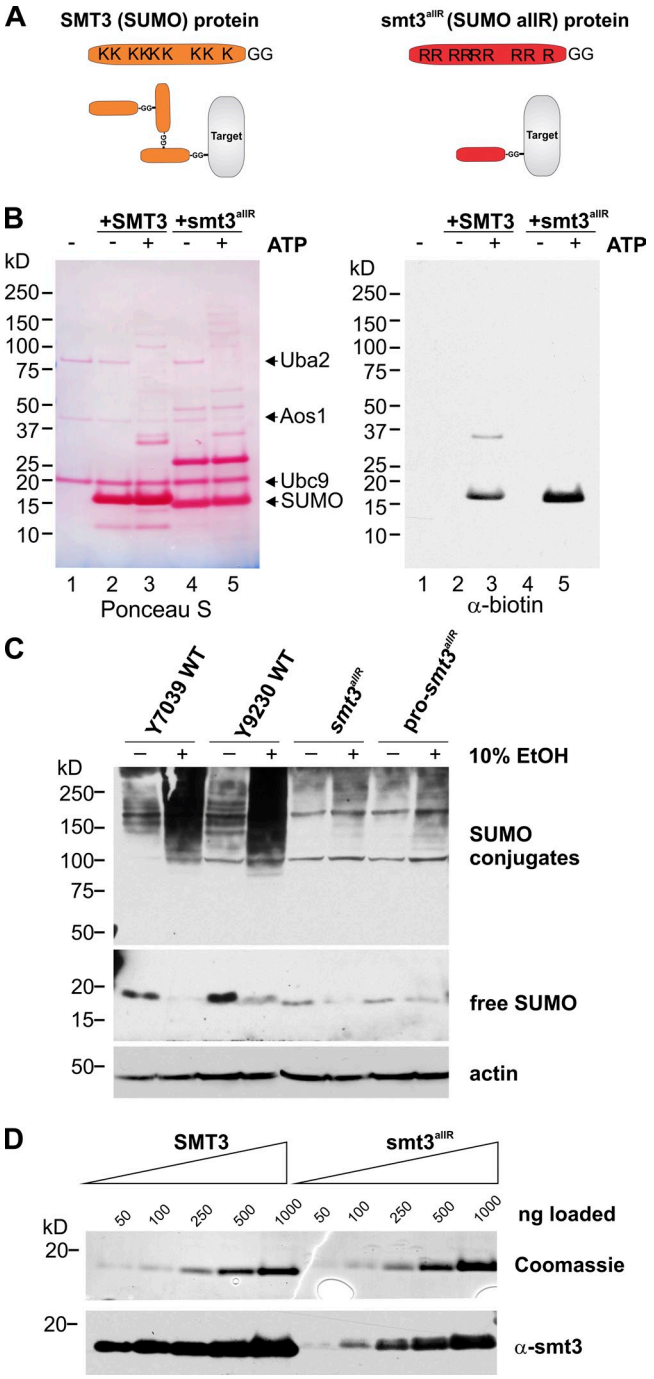

Figure 1. **A SUMO allR polypeptide can be conjugated to target proteins, but is unable to form SUMO chains in vitro and in vivo.** (A) Schematic representation of the WT SUMO and SUMO allR proteins. Although both SUMO protein variants can be covalently conjugated to substrates (also known as "target" proteins), the allR SUMO polypeptide lacks lysine residues, and is therefore unable to form SUMO chains. (B) WT SUMO and the SUMO allR protein are conjugated to a biotinylated polypeptide (a model substrate containing the sumoylation consensus sequence) at similar efficiencies in vitro. Reactions were conducted in the presence (+) and absence (−) of ATP. (Lane 1) SUMO E1 and E2 proteins, along with the biotinylated substrate peptide (reaction mix). (Lanes 2 and 3) Reaction mix plus WT SUMO protein. (Lanes 4 and 5) Reaction mix plus allR SUMO protein. (C) *smt3*^{allR} strains do not form high-molecular-weight SUMO conjugates in response to environmental stress. WT and *smt3*^{allR} cells were exposed to 10% ethanol (EtOH) for 1 h, and SUMO conjugates were visualized by Western blot analysis of whole cell lysates. Unconjugated SUMO is shown in the middle panel (a longer exposure of the same Western blot), and actin (loading control) in the bottom panel. The pro-*smt3*^{allR} strain expresses a SUMO allR pro-protein, which possesses three additional C-terminal residues that must be cleaved to generate the mature SUMO protein. The *smt3*^{allR} strain expresses a mature form of the allR SUMO protein. (D) The SUMO antibody does not detect the SUMO allR protein with the same efficiency as the WT SUMO polypeptide. Equal amounts of purified recombinant SUMO WT and allR proteins were subjected to Coomassie blue staining (top) and Western blotting (bottom).

an approximately twofold increase in cells with >2n DNA content (Fig. 2 B) in the *smt3*^{allR} cell population ($P < 0.01$). Consistent with observations in other SUMO pathway mutants (Felberbaum and Hochstrasser, 2008; Lee et al., 2011), DAPI staining revealed chromosome segregation defects in a subset of the *smt3*^{allR} population (~40% of large budded cells; Fig. 2 C and Fig. S1 A). A lack of SUMO chain synthesis thus appears to negatively affect the efficient segregation of chromosomes, which in turn leads to an increase in population ploidy.

Consistent with a role for SUMO chains in DNA replication, *smt3*^{allR} cells also displayed hypersensitivity to the ribonucleotide reductase inhibitor hydroxyurea (HU) and the alkylating agent methyl methanesulfonate (MMS), but did not exhibit increased sensitivity to DNA damage induced by zeocin or 4-nitroquinoline 1-oxide (4NQO; Fig. 2 D and Fig. S1 B), and did not display increased sensitivity to high or low temperatures, or protein-damaging agents (Fig. 2 D and Fig. S1, B and C).

Strikingly, untreated *smt3*^{allR} strains displayed a >10-fold increase in the number of steady-state DNA damage foci, as visualized via RAD52-GFP, DDC1-GFP, and RFA1-GFP (parental strain average for all markers = 1.51 ± 0.63 foci/field; *smt3*^{allR} average = 17.1 ± 2.93 foci/field; Fig. 2 E). To further explore the role of SUMO chains in replication-associated DNA damage, we crossed the *smt3*^{allR} strain with 384 yeast strains expressing GFP-tagged proteins (Huh et al., 2003) previously linked to the DNA damage response (Tkach et al., 2012). Live cells were imaged using automated high-throughput confocal microscopy (Tkach et al., 2012) and the resulting images were examined for differences in localization and signal intensity in the SUMO chain mutant (Table 1 and Table S1). This high content screen (HCS) highlighted changes in localization and/or intensity in *smt3*^{allR} cells for 144 proteins, most of which are involved in DNA replication, segregation, or repair processes (Table 1 and Table S1). These data are consistent with several earlier publications linking the SUMO system to replication stress (Branzei et al., 2006; Xiong et al., 2009), yet significantly expand the repertoire of DNA damage–associated proteins demonstrated to be affected in response to SUMO system defects. Most importantly, these data for the first time also specifically implicate SUMO chains in this function.

SMT3 was first characterized as a high-copy suppressor of *mif2*, a kinetochore protein required for structural integrity of the mitotic spindle (Meluh and Koshland, 1995; Vizeacoumar et al., 2010). Chromosomal passenger complex protein localization is also regulated by the SUMO system, to mediate spindle disassembly (Vizeacoumar et al., 2010). Consistent with a role for SUMO chains in mitotic spindle dynamics, the HCS highlighted

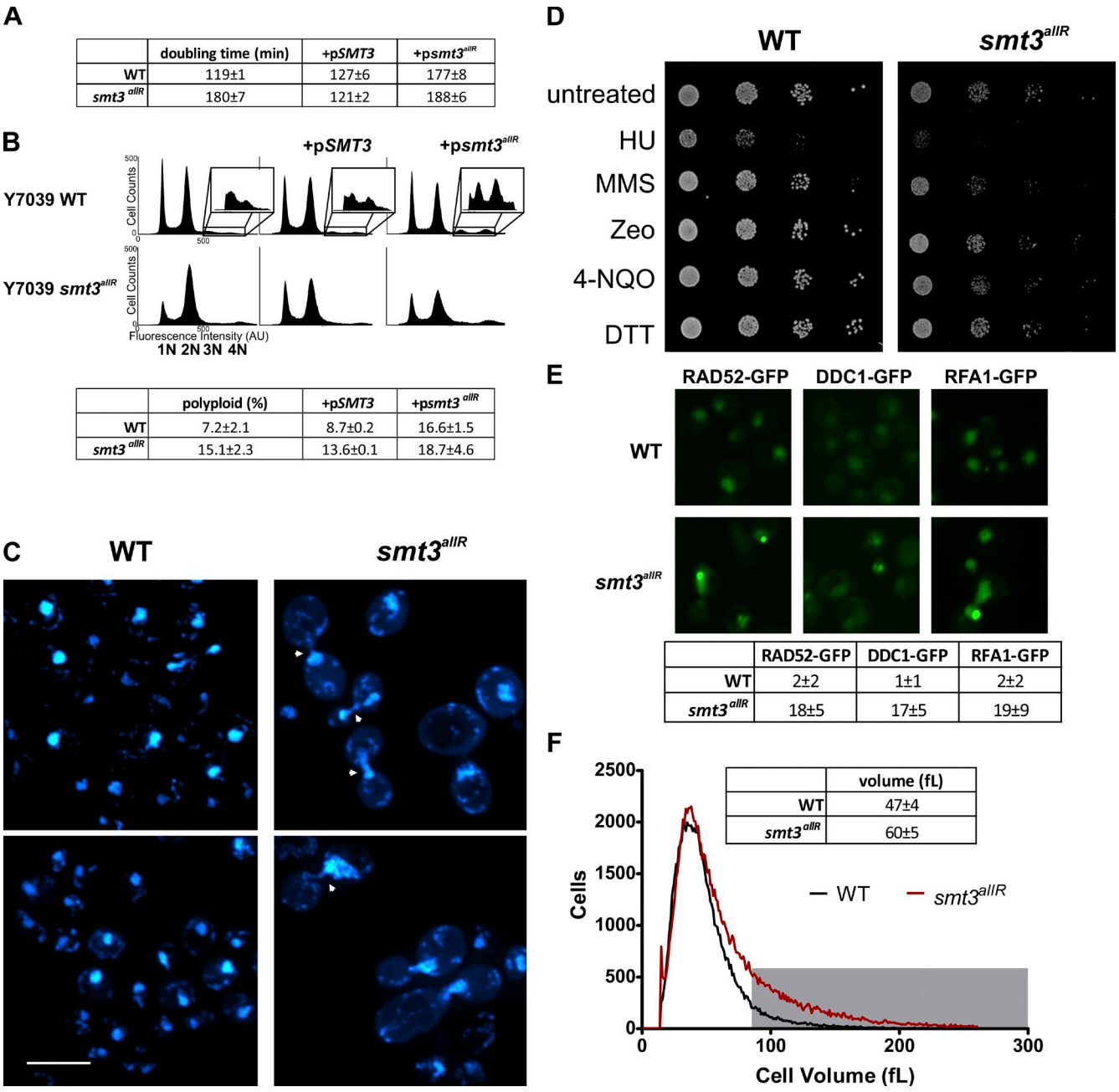

	doubling time (min)	+p*SMT3*	+p*smt3*^{allR}
WT	119±1	127±6	177±8
smt3 ^{allR}	180±7	121±2	188±6

	polyploid (%)	+p*SMT3*	+p*smt3* ^{allR}
WT	7.2±2.1	8.7±0.2	16.6±1.5
smt3 ^{allR}	15.1±2.3	13.6±0.1	18.7±4.6

	RAD52-GFP	DDC1-GFP	RFA1-GFP
WT	2±2	1±1	2±2
smt3 ^{allR}	18±5	17±5	19±9

	volume (fL)
WT	47±4
smt3 ^{allR}	60±5

Figure 2. ***smt3*^{allR} mutant yeast strains display increased doubling time, chromosome segregation defects, and increased ploidy, and are sensitive to DNA replication inhibitors.** (A) Doubling time (mean ± SD) was measured over an 8-h period of log-phase growth for *smt3*^{allR} and parental strains. Strains (as indicated) were also transfected with a galactose-inducible *SMT3* (WT) or *smt3*^{allR} plasmid (+p*SMT3* or +p*smt3*^{allR}, respectively), which was induced for 18 h before the first doubling time measurement. (B) FACS analysis of untransfected parental and *smt3*^{allR} strains, and the same strains expressing the WT or allR SUMO proteins (as in A). DNA was stained with SYTOX green and data were collected on 50,000 events. The insets highlight the polyploid (>2n) population in each analysis. (C) Parental and *smt3*^{allR} strains were stained with DAPI and imaged using confocal microscopy. Two representative images from each strain are shown. Cells displaying abnormal chromosome segregation are highlighted with arrowheads. Bar, 10 µm. (D) Log-phase cells were treated as indicated for 1 h, serially diluted (10×), and spotted onto YPD plates (HU, hydroxyurea; MMS, methyl methanesulfonate; Zeo, zeocin; 4-NQO, 4-nitroquinoline 1-oxide; DTT, dithiothreitol; Linger and Tyler, 2005; Rand and Grant, 2006; Tang et al., 2009). Colonies were grown for 2 d at 30°C. (E) Spontaneous DNA damage foci were quantified in parental and *smt3*^{allR} strains using GFP-tagged RAD52, DDC1, and RFA1. The mean number of foci (±SD) from four fields is tabulated. Bar, 10 µm. (F) Cell size distribution (mean ± SD) was measured on a Z2 counter (Beckman Coulter), as in Jorgensen et al. (2002). The gray box highlights the cell population with a volume >80 fL in the parental (black line) and *smt3*^{allR} (red line) strains. Data shown are from a single representative experiment, conducted twice.

mislocalization of several additional proteins (4 of 11 proteins in the screen) involved in spindle function (Table 1 and Fig. S2).

Also of note, although a majority of cells fell within the normal size range, a subpopulation of *smt3*^{allR} cells exhibited significant increases in volume ($P < 0.001$; Fig. 2 F). The proportion of cells with a volume >80 fl (more than two standard deviations from the mean) was 11 ± 4% for parental strains and 30 ± 6% for *smt3*^{allR} strains. Both large and normal sized *smt3*^{allR}

Table 1. ***smt3^{allR}* HCS**

Group	Protein								
DNA replication and repair	AQR1	DPB11	HST4	MGS1	NUP53	RAD59	RPL40A	SLD3	XRS2
	CGR1	DUN1	IPL1	MKT1	PNC1	RFA1	RPN4	SLX4	YDL156W
	DBF4	DUS3	LCD1	MRE11	RAD50	RFA2	SAE2	STP1	YJR056C
	DDC1	GLN1	MCM2	MRS6	RAD52	RFC2	SGF11	TRM112	YML108W
	DNA2	SRS2	MCM4	MSN2	RAD57	RNR4	SGS1	TSR1	ZPR1
Polarization/budding/bud site selection	BUD14	GSP2	MSB1	NBA1	CDC24	GYL1	MSB3	OPY2	
Ion homeostasis (pH)	ARN1	CTR1	VMA10	VMA4	YLR126C	YOL092W	CRD1	POR1	VMA2
	VPH1	YML018C							
mRNA catabolic processes	DCP1	EDC2	LSM1	LSM3	LSM7	NMD4	PBP4	DHH1	EDC3
	LSM2	LSM4	NAM7	PAT1					
Spindle defects	ASE1	DAD3	CNM67	DAD4					
Vacuole function	LAP4	PEP8	VPS1	YLR297W	MTC5	PIB1	YIR014W		
Ribosome biogenesis	ATC1	CMS1	GDT1	NOP13	RMT2	ATG29	ECM1	HGH1	NOP58
	RPL7B								
Stress response	AHA1	CUE1	HSP42	ITR1	TSA1	YKL069W	APJ1	GSY2	HXT3
	SCH9	WSC4							
Cell shape defects	DSE3	NEO1	SEC10	SEC6	VPS41	FLC1	RAS1	SEC3	SEC8
Other	ATG16	FAT1	KTR3	PBY1	PPH21	SRP68	YDL085C-A	YGR042W	YKR011C
	CHS7	HOM6	LSB1	PEX21	RSM10	YBR259W	YDR090C	YHR140W	YLR363W-A
	FAA1	IRC22	MDM12	PIL1	SGT2	YDC1	YDR170W-A	YIL108W	YMR111C

144 GFP-tagged proteins displayed a change in localization and/or intensity when expressed in the *smt3^{allR}* mutant grown in rich medium. Proteins are grouped according to ten functional categories.

cells successfully produced colonies, and gave rise to a mix of normal and large cells in similar proportions (unpublished data), which indicates that the large cell phenotype is neither terminal nor heritable. The size increase thus likely reflects a cell cycle delay caused by an increased DNA repair load and chromosome segregation defects.

smt3^{allR} cells display characteristics of an activated environmental stress response

The HCS also highlighted several GFP-tagged vacuolar proteins with clear changes in localization in *smt3^{allR}* cells; e.g., VPS1-GFP and VPS41-GFP displayed more numerous puncta than parental cells (Fig. S2). Multiple mitochondrial markers (e.g., MDM12-GFP and POR1-GFP) also displayed markedly increased signal intensity in the *smt3^{allR}* strains (Fig. S2). Consistent with these data, electron micrographs revealed a large subset of *smt3^{allR}* cells with fragmented vacuoles, increased mitochondrial volume, and thicker cell walls than parental strains (Fig. 3 A and Fig. S3 A). These defects were unexpected and were investigated further.

Signal intensities for a GFP bearing a mitochondrial targeting sequence (Westermann and Neupert, 2000) and Mitotracker red, a thiol-reactive dye that accumulates in active mitochondria, were strikingly enhanced in cells defective for SUMO chain synthesis (Fig. 3 B). *smt3^{allR}* cells also exhibited a significant increase (more than fourfold; $P < 0.01$) in basal oxygen consumption rates (Fig. 3 C), even when maintained in glucose-containing culture media (a condition in which glycolysis is the preferred mode of energy production). *smt3^{allR}* cells thus maintain abnormally high levels of mitochondria that are metabolically active even in the presence of glucose.

Vacuolar fragmentation is observed in cells in a hypertonic environment (Ryan et al., 2008). Glycerol is the primary osmoprotectant in *S. cerevisiae*, and is synthesized in response to hyperosmotic conditions to maintain cell turgor (Hohmann, 2009). *smt3^{allR}* cells grown in isosmotic media displayed highly fragmented vacuoles and a more than twofold increase ($P < 0.01$) in intracellular glycerol concentrations, as compared with parental strains (Fig. S3, B and C). These data suggest that SUMO chain mutants are also subject to chronic osmotic stress or exhibit aberrant osmotic stress signaling.

Together, our data reveal that disruption of SUMO chain assembly gives rise to a pleiotropic cell population exhibiting several different physiological defects. We did not observe any clear correlation between, e.g., ploidy and the number of DNA damage foci or mitochondrial mass, which suggests that these phenotypes are largely independent of one another.

Replication-associated DNA damage is observed in other types of SUMO system mutants (Branzei et al., 2006; Schwartz et al., 2007), and our analysis implicates SUMO chains in this process. However, we also observed phenotypic characteristics in *smt3^{allR}* cells that have not previously been described for other types of SUMO mutants. Many of these traits are reminiscent of an inappropriately activated response to environmental stress or nutrient-poor media conditions.

The *smt3^{allR}* phenotype is caused by a lack of SUMO chains

To confirm that the *smt3^{allR}* phenotype is caused by a lack of SUMO chains, and not to secondary mutations that could arise in such mutants, we transformed plasmids coding for galactose-inducible WT or allR SUMO proteins into parental and *smt3^{allR}* strains, and assessed their effects on doubling time, ploidy, and

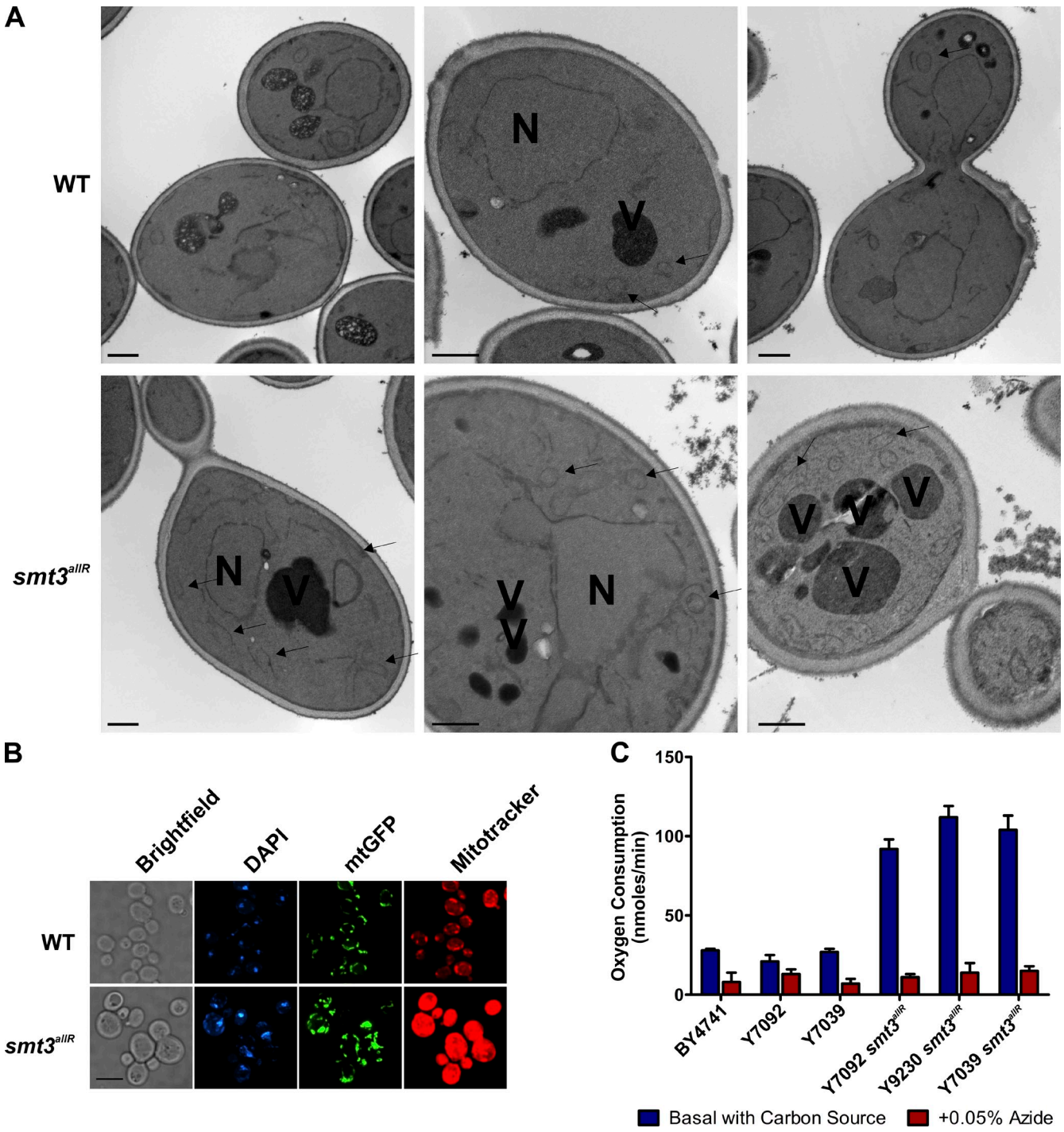

Figure 3. **Ultrastructural characterization of *smt3*^{allR} mutant strains.** (A) Electron micrographs of parental and *smt3*^{allR} cells, highlighting the nucleus (N), vacuoles (V), and mitochondria (arrowheads). Bars, 500 nm. (B) Mitochondrial-targeted GFP (mtGFP) and MitoTracker red CMXRos staining highlight increased mitochondrial volume in *smt3*^{allR} mutant cells. (C) Basal oxygen consumption of parental and *smt3*^{allR} mutant cells (error bars indicate mean ± SD) grown in YPD. Azide treatment inactivates oxidative respiration and indicates levels of nonmitochondrial oxygen consumption.

vacuolar morphology. Additional SUMO allR protein expression in the *smt3*^{allR} strain (induced for 16 h) had no apparent effect on cycling time (188 ± 6 min), ploidy, or vacuole size and number (Fig. 2, A and B; and Fig. S3 D). Similarly, overexpression of the WT SUMO protein in parental strains had no discernible effect on these phenotypic features (Fig. 2, A and B; and Fig. S3 D). However, overexpression of the SUMO allR protein in parental (WT) strains led to a significant increase in doubling time (177 ± 8 min, $P < 0.001$; Fig. 2 A), an increase in the number of cells with >2n DNA ploidy (Fig. 2 B), and an increase in vacuolar fragmentation (Fig. S3 D). Conversely, expression of the WT SUMO protein in *smt3*^{allR} strains led to a decrease in doubling time (121 ± 2 min, $P < 0.001$), a decrease in the proportion of cells with >2n DNA ploidy, and a decrease

in vacuolar fragmentation (Fig. 2, A and B; and Fig. S3 D). The *smt3*^{allR} phenotype can thus be at least partially rescued by expression of a SUMO protein that can form chains, and overexpression of the SUMO allR protein in WT cells can effect changes in cycling time, ploidy, and vacuolar morphology even in the presence of the endogenous SUMO polypeptide. Together, these data indicate that the *smt3*^{allR} phenotype is not caused by a limited supply of the SUMO protein for conjugation, or to secondary mutations in these strains, but is indeed caused by a lack of SUMO chains. These data also demonstrate that the SUMO allR protein can act in a dominant manner in the presence of the endogenous SUMO polypeptide, presumably by preventing SUMO chain formation.

Previous studies have indicated that SUMO chains in vivo are linked primarily via N-terminal lysine residues (mostly through K15; Bencsath et al., 2002). To determine whether the *smt3*^{allR} phenotype could be recapitulated by disrupting only the N-terminal lysine residues, we also expressed a SUMO 3KR mutant (in which only lysines 11, 15, and 19 are mutated to arginine residues) in WT cells. Division time and ploidy were indistinguishable from cells expressing the SUMO allR mutant (Fig. S4), which further suggests that the *smt3*^{allR} phenotype is caused by the disruption of SUMO chains. In the remaining work presented here, we used *smt3*^{allR} strains to avoid any possibility of SUMO chain synthesis via the use of alternative lysine residues (as we and others have observed in vitro; Bencsath et al., 2002; Bylebyl et al., 2003; Jeram et al., 2010).

A SUMO chain genetic interaction network

To identify cellular pathways that specifically compensate for disrupted SUMO chain synthesis, the *smt3*^{allR} strain was subjected to synthetic genetic array (SGA) analysis, as in Makhnevych et al. (2009) and Costanzo et al. (2010). The *smt3*^{allR} mutant was crossed with an ordered array of ∼4,700 viable yeast deletion mutants, and the resulting strains were scored for colony growth (Baryshnikova et al., 2010). To avoid the possibility of false-positive interactions caused by secondary mutations in the SUMO chain mutant, SGA was conducted twice, using two different *smt3*^{allR} strains (one expressing pro-SMT3^{allR} and one expressing the mature SMT3^{allR} polypeptide, as in Fig. 1 C). 149 high-confidence synthetic genetic interactions were detected in both analyses (Table S2). The resultant SUMO chain genetic interaction network represents the first global genetic analysis of SUMO chain function in any organism. Gene ontology (GO) analysis (Table S2) highlighted significant enrichment in interactions with genes involved in DNA replication, DNA damage repair, chromatin remodeling, cell cycle control, stress responses, protein catabolism, nuclear transport, and meiosis.

SGA correlation analysis (i.e., the comparison of genetic interaction maps) is useful for gaining insight into the function of a gene of interest, because genes that share similar patterns of genetic interactions are likely to share similar biological roles (Costanzo et al., 2010). The *smt3*^{allR} SGA profile was thus compared with SGA-derived genetic interaction profiles of 4,458 mutant strains available in the data repository of the yeast genetic interactions database (DRYGIN; Koh et al., 2010). 194 genes displayed a significant positive correlation with the *smt3*^{allR} genetic interaction map (Fig. 4, Table 2, and Table S2). Attesting to the robustness of this analysis, three of the four highest correlated genes were derived from components of the SUMO system itself: *ubc9* (*ubc9-2*), *mms21* (*mms21-sp*), and *smt3* (smt3-damp; decreased abundance by mRNA perturbation; Yan et al., 2008). *ulp1* was also a top-scoring hit (*ulp1-333*). Likely reflecting a role in a subset of SUMO functions, *siz2* (*nfi1*) displayed a significant, but lower, overlap with the *smt3*^{allR} interaction profile. Consistent with STUbL-mediated degradation as a major function for SUMO chains, the second most highly correlated genetic interaction map in our screen was *slx8*. The gene coding for its binding partner *slx5* was also a top-scoring hit.

As expected, ubiquitin-proteasome system (UPS) components were also highlighted in this analysis; the UPS works with Slx5-Slx8 to effect SUMO-targeted protein degradation. We also observed overlap with the *cdc48* (p97) SGA map. This protein was recently reported to work with the Slx5-Slx8 proteins to mediate genome stability (Nie et al., 2012). Another set of highly correlated genes corresponded to nuclear pore complex (NPC) components and karyopherins (*nup60*, *nup133*, *nup145-R4*, *nup84*, and *srp1-damp*). This is also not unexpected, as strains with a loss of function in any of these genes display aberrant Ulp1 localization, which directly impacts SUMO system function (Panse et al., 2003; Makhnevych et al., 2007).

Consistent with the *smt3*^{allR} phenotype, several proteins involved in DNA replication and repair shared significant similarity with the *smt3*^{allR} genetic interaction profile, including several DNA polymerases, helicases, and exonucleases (e.g., *rad27*, *cdc2-1*, *pol32*, *pol12-ts*, *pol1-13*, *rrm3*, etc.), and genes implicated in stalled replication fork stabilization (e.g., *tof1*, *mrc1*, and *csm3*, and the MCM helicase complex: *mcm3-1*, *cdc47-ts*, and *cdc46-1*). Recent work has also demonstrated that the SUMO E3 ligase Mms21, as part of the Smc5-6 complex, plays a critical role in resolving recombination intermediates at damaged DNA templates (Branzei et al., 2006; Chavez et al., 2010). Smc5-6 mutants undergo aberrant mitosis, in which chromosome segregation of repetitive regions is impaired (Torres-Rosell et al., 2005). A failure to resolve this type of DNA damage can lead to chromosomal rearrangements and increased ploidy. Indeed, multiple components of the Smc5-Smc6 complex (*mms21-1*, *nse3-ts4*, *nse4-ts2*, *kre29-ts2*, etc.) were highly correlated in our analysis. Also as observed in our HCS, genetic interaction maps for *esc2*, *sgs1*, *mus84*, and *mms1*, all of which play an important role in resolving homologous recombination repair DNA intermediates in response to replication stress (Ashton and Hickson, 2010; Rossi et al., 2010; Hickson and Mankouri, 2011), were highly correlated with the *smt3*^{allR} interaction map.

Notably, SGA correlation analysis also highlighted similarity between *smt3*^{allR} and several proteins involved in chromatin organization and remodeling. For example, significant correlations were observed with the histone chaperone *asf1*, several components of chromatin assembly factor-1 (CAF-1; *cac2*, *rlf2*, and *msi1*), the histone acetyltransferase *rtt109*, the histone H2A.Z exchange complex SWR1 (*swr1*, *vps71*, *arp6*, *swc4-4*, etc.), histone deletants (*hta1*, *htz1*, *hhf1*), and *spt21* (required for proper histone gene transcription).

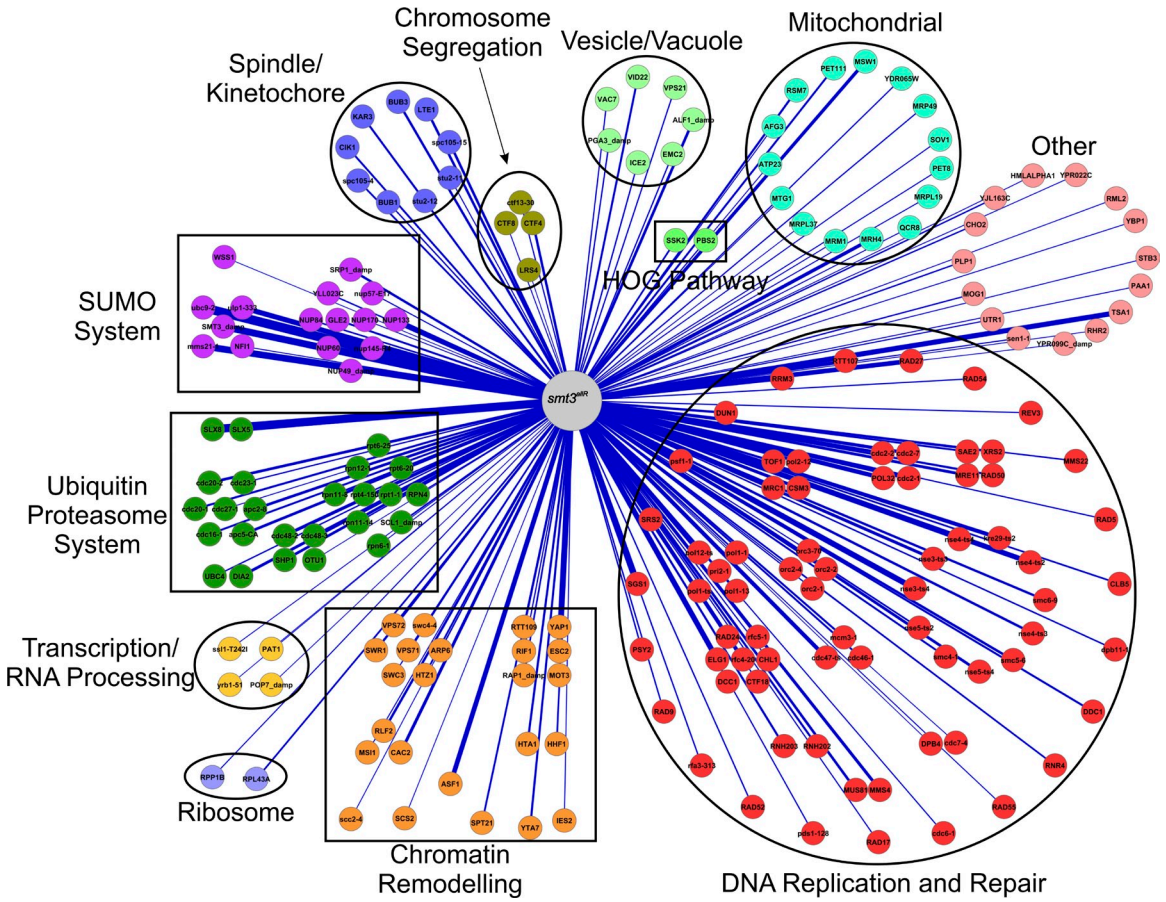

Figure 4. ***smt3^{allR}* SGA correlation analysis.** 194 genes yielded a significant positive correlation with the *smt3^{allR}* genetic interaction network. Edge width corresponds to correlation values.

Interestingly, we also observed similarity with genes implicated in mitochondrial function (e.g. *mrh4*, *msw1*, and *mrp49*) and osmotic stress signaling (*ssk2* and *pbs2*). Consistent with our HCS data and several previous publications linking the SUMO system to spindle function (Vizeacoumar et al., 2010; Pérez de Castro et al., 2011; Wan et al., 2012), SGA correlation analysis also highlighted several spindle and kinetochore genes (e.g., *bub3, spc105-15, lte1*, *kar3*, *clk1*, *stu2-11*, and *stu2-12*).

In sum, our genetic data implicate SUMO chains in several functions previously ascribed to the SUMO system, such as resolving DNA replication–associated repair structures, but also link them to some previously unsuspected biological roles, such as osmoregulation and higher order chromatin structure.

Derepression of stress- and nutrient-regulated gene transcription and aberrant transcription of cryptic intergenic regions in *smt3^{allR}* strains

High-resolution whole genome nucleotide tiling arrays (see Materials and methods for details) were next used to characterize the transcription profile of cells defective for SUMO chain synthesis (as in Tsui et al., 2012). 36 genes were repressed and 225 mRNAs were expressed >1.5-fold higher in the *smt3^{allR}* strain, as compared with parental cells (Table 3 and Table S3). The up-regulated mRNAs consisted primarily of genes implicated in stress responses, nutrient adaptation, cell wall components, mitochondrial proteins, sporulation, and mating; i.e., genes that are normally repressed under standard laboratory culture conditions, where cells are maintained in media with optimal carbon and nitrogen sources, and at optimal growth temperature. Increased transcription of this gene set likely accounts for many aspects of the pleiotropic *smt3^{allR}* phenotype. For example, several genes implicated in mitochondrial function (e.g., *STF1*, *ALD4*, and *CYC7*) and cell wall integrity signaling (e.g., *YGP1*, *KDX1*, and *PRM5*) are up-regulated in this strain. These data suggest that SUMO chains are likely to be involved indirectly in each of these biological functions, via transcriptional control.

We also observed a notable increase in transcription from silenced mating type and sporulation genes (e.g., *MFA1*, *MFA2*, *RIM4*, and *PRM1*), as well as several intergenic regions (Fig. S5 A and Table S3); e.g., 47 cryptic unstable transcripts (CUTs) were expressed >1.5-fold higher in the *smt3^{allR}* strain than in parental cells. Together, these data indicate that disruption of SUMO chain synthesis has a wide-ranging negative effect on the maintenance of transcriptional repression. (It should also be noted that, although overall changes in the expression of individual transcripts are not extremely large in these mutants, this number reflects a population average. Because the phenotypes of individual *smt3^{allR}* cells are pleiotropic, we suspect that these averages reflect much larger changes in a smaller subpopulation of cells.)

Table 2. ***smt3^{allR}* SGA correlation analysis**

Category	Gene	Correlation
SUMO system		
SUMO system components	ubc9-2	0.430
	SMT3_damp	0.338
	mms21-1	0.329
	ulp1-333	0.263
	NFI1	0.087
NPC components–Ulp1 localization	NUP60	0.328
	NUP133	0.228
	nup145-R4	0.223
	SRP1_damp	0.149
	NUP84	0.113
	GLE2	0.130
	YLL023C	0.109
	nup57-E17	0.094
	NUP49_damp	0.091
Chromatin remodeling		
Histone chaperone	ASF1	0.247
Chromatin silencing	ESC2	0.294
	RTT109	0.141
	RAP1_damp	0.116
	MOT3	0.110
	YAP1	0.109
	RIF1	0.099
Chromatin assembly factor (CAF-1)	CAC2	0.176
	RLF2	0.148
	MSI1	0.090
Histones	HTA1	0.139
	HTZ1	0.123
	HHF1	0.119
SWR1 complex	SWR1	0.144
	HTZ1	0.123
	VPS71	0.108
	ARP6	0.105
	swc4-4	0.099
	VPS72	0.098
	SWC3	0.097
DNA replication and repair		
MRX complex	MRE11	0.166
	XRS2	0.154
	RAD50	0.138
	SAE2	0.127
MCM complex	cdc47-ts	0.217
	mcm3-1	0.132
	cdc46-1	0.127
Mms21–Smc5–Smc6 complex	mms21-1	0.329
	nse3-ts4	0.287
	nse4-ts2	0.263
	kre29-ts2	0.213
	nse4-ts4	0.183
	nse3-ts3	0.175
	nse5-ts4	0.165
	smc5-6	0.152
	nse4-ts3	0.151
	smc6-9	0.147
	nse5-ts2	0.118
Pol2–TOF1–MRC1–CSM3 complex	MRC1	0.206
	pol2-12	0.182
	CSM3	0.180
	TOF1	0.141
Origin recognition complex	orc2-2	0.157
	orc2-4	0.096
	orc3-70	0.095
Ribonuclease 2	RNH203	0.138
	RNH202	0.137
Polymerase delta	POL32	0.231
	cdc2-1	0.219
	cdc2-7	0.185
	cdc2-2	0.167
Mms4–Mus81 complex	MMS4	0.177
	MUS81	0.156
Pol1-DNA primase	pol12-ts	0.192
	pol1-13	0.128
	pol1-ts	0.120
	pol1-1	0.118
	pri2-1	0.109
RFC complex	ELG1	0.271
	rfc4-20	0.214
	rfc5-1	0.153
	RAD24	0.116
	CTF18	0.101
	CHL1	0.097
	DCC1	0.092
Other	RAD27	0.242
	RRM3	0.192
	RTT107	0.168
	psf1-1	0.158
	DUN1	0.146
	DDC1	0.133
	RNR4	0.120
	CLB5	0.119
	RAP1_damp	0.116
	dpb11-1	0.111
	MMS22	0.108
	RAD5	0.100
	RAD54	0.098
	REV3	0.098
	RAD17	0.097
	cdc6-1	0.097
	RAD55	0.090
Ubiquitin–proteasome system		
STUbL	SLX8	0.393
	SLX5	0.247
Cdc48	cdc48-2	0.183
	SHP1	0.160
	cdc48-3	0.145
	OTU1	0.081
APC/C	apc5-CA	0.162
	apc2-8	0.161
	cdc20-2	0.161
	cdc20-1	0.134
	cdc16-1	0.130
	cdc23-1	0.102
SCF	DIA2	0.169
	UBC4	0.105
Proteasome	rpn12-1	0.155
	rpn11-8	0.127

Table 2. ***smt3^{allR}* SGA correlation analysis** *(Continued)*

Category	Gene	Correlation
	SCL1_damp	0.118
	rpn11-14	0.107
	rpt1-1	0.107
	RPN4	0.100
	rpt6-20	0.091
Miscellaneous		
Spindle/kinetochore	spc105-15	0.154
	LTE1	0.152
	BUB3	0.149
	KAR3	0.135
	CIK1	0.129
	CLB5	0.119
	BUB1	0.105
	stu2-12	0.094
	stu2-11	0.092
HOG pathway signaling	SSK2	0.120
	PBS2	0.082
Vesicle/vacuole	ALF1_damp	0.160
	LTE1	0.152
	VID22	0.133
	ICE2	0.105
	PGA3_damp	0.104
	EMC2	0.102
	VPS21	0.101
Mitochondrial function	MRH4	0.193
	MSW1	0.187
	PET111	0.131
	MRP49	0.100
	YDR065W	0.100
	PET8	0.092
	SOV1	0.092
	QCR8	0.090
	MRPL19	0.090

194 genes display a positive correlation with the *smt3*^{allR} genetic map. Genes are grouped according to functional categories.

SUMO chains are required to establish a basal transcription "setpoint" for stress-regulated genes

The transcription of stress-response genes is rapidly increased in response to changes in the extracellular environment (Gasch et al., 2000). To explore the role of SUMO chains in the transcriptional stress response, we subjected parental and *smt3^{allR}* cells to hyperosmotic culture conditions (1 M NaCl for 30 min), followed by a 120-min recovery in isosmotic media. Using real-time qRT-PCR, expression levels of four different mRNAs that are overexpressed in *smt3^{allR}* cells, and which are up-regulated in response to osmotic shock (*HSP12*, *SPS100*, *GRE1*, and *HUG1*), were monitored. As expected, in parental cells all four of the genes in the test set displayed a rapid increase in mRNA levels in response to hyperosmotic shock (Fig. 5 and Fig. S5 B). After a return to isosmotic media, a gradual decrease in mRNA abundance was observed, returning to pre-stress levels within 60–120 min (Fig. 5 and Fig. S5 B). Consistent with our tiling array data, this gene set was already expressed at higher levels in untreated *smt3^{allR}* strains (Fig. 5 and Fig. S5 B). In response to osmotic shock, the four gene set was up-regulated to approximately the same expression levels (or slightly higher in some cases) as the parental strain, and removal of the stress resulted in a similar gradual decrease in mRNA abundance to near basal *smt3^{allR}* transcript levels (Fig. 5 and Fig. S5 B). Identical results were observed in cells expressing the 3KR SUMO protein (Fig. S4 C). A deficiency in SUMO chain function does not therefore appear to significantly affect the activation kinetics or maximal mRNA expression levels in response to stress, but instead influences the basal transcription setpoint of this highly regulated group of genes.

SUMO chain disruption affects multiple aspects of higher-order chromatin organization

Aberrant mitotic chromosome condensation and segregation, transcriptional derepression of stress- and nutrient-regulated genes, and aberrant transcription from intergenic regions suggested that *smt3^{allR}* strains could have a chromatin condensation defect. To this end, we subjected *smt3^{allR}* and parental cells to several different assays of higher-order chromatin structure.

The lacO/lacR chromosome marker system. To begin to assess how a lack of SUMO chains impacts chromatin structure, we used a yeast strain bearing two lac operon repeat insertions on chromosome IV, separated by ∼450 kb (strain AVY89; Vas et al., 2007). When the lacR-GFP protein is bound to its cognate operon, confocal microscopy can be used to measure the distance between the two GFP foci (Vas et al., 2007). Plasmids encoding the gal-inducible WT or allR SUMO proteins were transformed into this strain, cells were exposed to galactose to induce SUMO protein expression for 16 h, and cells were treated with α factor to synchronize them in G1. The distance between GFP signals was then quantified, as in Vas et al. (2007). In cells expressing the WT SUMO protein, the two GFP foci were 1.19 ± 0.04 µm apart on average, the same as that observed in the untransformed parental strain (Fig. 6, A and B) and similar to measurements previously reported in other laboratory strains (Vas et al., 2007). Notably, in the strain expressing the SUMO allR protein, the mean distance between the GFP-marked chromosome regions was significantly increased (1.45 ± 0.05; $P < 0.01$; Fig. 6, A and B). Inhibition of SUMO chain formation thus negatively affects chromosome IV compaction and/or organization.

Telomere clusters. The SUMO system was also previously linked to telomere silencing and localization (Chen et al., 2007; Mekhail et al., 2008; Ferreira et al., 2011). During interphase, budding yeast telomeres are clustered into 3–8 foci located near the inner nuclear membrane (INM; Mekhail et al., 2008). To determine if SUMO chains are important for proper telomere organization, we examined the localization of the telomere regulatory protein SIR2 in parental and *smt3^{allR}* strains. As expected, in parental strains, SIR2-GFP was found in a small number of foci near the INM. However, *smt3^{allR}* cells displayed an increased number of (generally smaller) SIR2-GFP foci, and many cells possessed an additional diffuse nuclear SIR2 signal (Fig. 7 A), which indicates widespread SIR2 mislocalization.

Nucleolar chromatin organization. The ribosomal DNA (rDNA) genes occur in a tandem array of ∼150 copies in

Table 3. ***smt3^{allR}* tiling array gene expression analysis**

Category	Gene	log_2 (fold change)	Gene	log_2 (fold change)	Gene	log_2 (fold change)	Gene	log_2 (fold change)	Gene	log_2 (fold change)	Gene	log_2 (fold change)	Gene	log_2 (fold change)
Nutrient/stress response														
	HSP12	2.912	HSP104	1.229	ECM4	0.954	SPG4	0.765	HMX1	0.606	DDR2	2.872	ALD3	1.200
	MOH1	0.933	TPS2	0.756	YMR090W	0.602	HSP26	2.805	SOL4	1.159	HOR2	0.907	DUR1,2	0.753
	MSN4	0.602	HUG1	2.404	CRG1	1.139	USV1	0.898	HSP31	0.746	PHO12	–0.602	TMA10	1.817
	ADR1	1.133	TMA17	0.896	RNY1	0.741	PHO11	–0.604	MSC1	1.803	NTH1	1.131	UBC5	0.893
	YOR052C	0.731	SPL2	–0.660	TSL1	1.793	ATG8	1.129	HOR7	0.882	YJL144W	0.711	ZRT1	–0.760
	GAD1	1.753	CTT1	1.104	PUT1	0.874	AHA1	0.691	RSN1	–0.805	HSP42	1.664	FRE7	1.045
	SOM1	0.860	YNR014W	0.677	AAH1	–0.805	GLK1	1.635	PRB1	1.037	ATH1	0.852	YNL134C	0.676
	PHM6	–0.815	TFS1	1.522	NCE103	1.036	SSA3	0.833	GRX1	0.664	HMS2	–0.832	PNC1	1.470
	GTT1	1.022	IGD1	0.826	EDC2	0.637	SSA4	1.465	SSE2	1.009	YJR096W	0.811	SPI1	0.631
	GRE1	1.394	GAC1	1.004	TPS1	0.808	RAD51	0.630	GCY1	1.382	PLM2	0.990	GPD1	0.802
	RCN2	0.630	HSP78	1.338	MCR1	0.980	GRE3	0.800	YAP6	0.628	PGM2	1.317	YDL124W	0.968
	CAR2	0.796	PEP4	0.620	XBP1	1.304	PRX1	0.966	PUT4	0.784	YOR289W	0.614	YDR034W-B	1.255
	SDS24	0.962	YKL151C	0.771	DAN4	0.609								
Mating and sporulation														
	AGA2	2.532	GPG1	1.320	CWP1	1.064	EMI2	0.694	TPK1	0.606	MFA1	1.555	PRM1	1.227
	BAR1	1.034	GSM1	0.678	PST2	0.604	HBT1	1.552	UBI4	1.223	PRM6	0.931	SPO12	0.651
	TCB2	–0.726	FIG1	1.450	FIG2	1.195	RMD5	0.784	FUS1	0.642	PRM7	–0.945		
	GSC2	1.377	AFR1	1.145	YOR338W	0.755	AGA1	0.641	RIM4	1.363	PRM2	1.108	FUS2	0.737
	PTP2	0.628	MFA2	1.345	STE2	1.102	KAR4	0.712	SPS100	0.616				
Carbohydrate metabolism														
	GPH1	2.447	HXT6	1.136	GND2	0.789	PFK26	0.679	HXK1	1.863	HXT7	1.130	YBR056W	0.723
	YLR345W	0.673	AMS1	1.699	GSY2	1.056	HXT5	0.720	RKI1	–0.616	NQM1	1.423	PIG1	0.914
	CIT1	0.717	HXT1	–0.710	GPM2	1.278	GSY1	0.868	UGP1	0.695	GDB1	1.252	GIP2	0.842
	PYK2	0.695	GLC3	1.192	PCK1	0.789	GUT2	0.689						
Cell wall														
	YGP1	2.467	KDX1	1.176	YPS6	1.017	DSE1	–0.650	EGT2	–0.718	YPS5	1.204	PRM5	1.103
	PIR3	0.988	SUN4	–0.685	PRY3	–1.042								
Autophagy														
	LAP4	1.229	DCS1	0.981	ATG34	0.878	PAI3	0.738	DCS2	1.025	ALD2	0.892	ATG33	0.743
	ATG19	0.732												
Mitochondrial														
	FMP16	1.902	CYC7	1.036	AIM17	0.984	MRP8	0.702	COX5B	0.656	CTP1	–0.806	STF1	1.622
	INH1	0.993	OM45	0.918	UIP4	0.699	MPM1	0.644	ALD4	1.305	FMP33	0.986	YNL200C	0.892
	GOR1	0.664	SDH2	0.633										
Other														
	YPR160W-A	2.593	YDR042C	1.159	VMR1	0.901	YMR181C	0.747	PIC2	0.641	SFG1	–0.605	YGL101W	–0.823
	YIL082W	2.021	YJL133C-A	1.145	LEE1	0.901	YLR312C	0.732	YNL058C	0.637	LIA1	–0.614	YBR191W-A	–0.862
	RTN2	1.860	ROM1	1.143	YOR343C	0.867	YBR139W	0.726	YPL088W	0.632	BSC1	–0.615	YMR317W	–0.907
	YMR196W	1.797	BOP2	1.142	PET10	0.858	YOR192C-C	0.709	YHR052W-A	0.624	NIP7	–0.629	PLB2	–0.923
	NCA3	1.724	CRG1	1.139	YLR307C-A	0.822	YER053C-A	0.692	YPR145C-A	0.623	LYS1	–0.633	YMR046W-A	–1.003
	RNR3	1.683	RTS3	1.115	YLR108C	0.798	COS12	0.690	YCL076W	0.622	HTB2	–0.654	YOL014W	–1.206
	PHM8	1.500	GSP2	1.097	PRY1	0.787	BNA2	0.685	PEX27	0.617	YBL029W	–0.688	YFR052C-A	1.498
	YKR011C	1.053	YDL247W-A	0.783	GAP1	0.684	YLR042C	0.617	YPR002C-A	–0.708	YNR034W-A	1.365	PBI2	0.993
	YBR201C-A	0.780	YOR114W	0.673	VPS73	0.614	ADE17	–0.712	RTC3	1.332	SRL3	0.987	CUR1	0.769
	YNL115C	0.670	REC104	0.611	HTA2	–0.719	YHR138C	1.263	ECL1	0.986	YCL021W-A	0.767	GGA1	0.663
	YHR007C-A	0.608	YNL217W	–0.729	YLR149C	1.179	YCL042W	0.954	YDR379C-A	0.758	HER1	0.657	RGC1	0.603
	ARG8	–0.764	YBR085C-A	1.178	BTN2	0.926	YCL049C	0.758	YBR053C	0.652	YHR177W	0.602	YDL038C	–0.799

High-resolution gene expression analysis of the *smt3^{allR}* mutant revealed that 261 genes were over- or underexpressed as compared to parental cells.

budding yeast laboratory strains, comprising ~1 Mb of chromosome XII (Johzuka and Horiuchi, 2009), and are organized into a compact structure localized near the INM, the nucleolus (Chan et al., 2011). Transcription of rDNA is tightly controlled, and specialized silencing mechanisms are required to prevent homologous recombination between rDNA repeats and to maintain

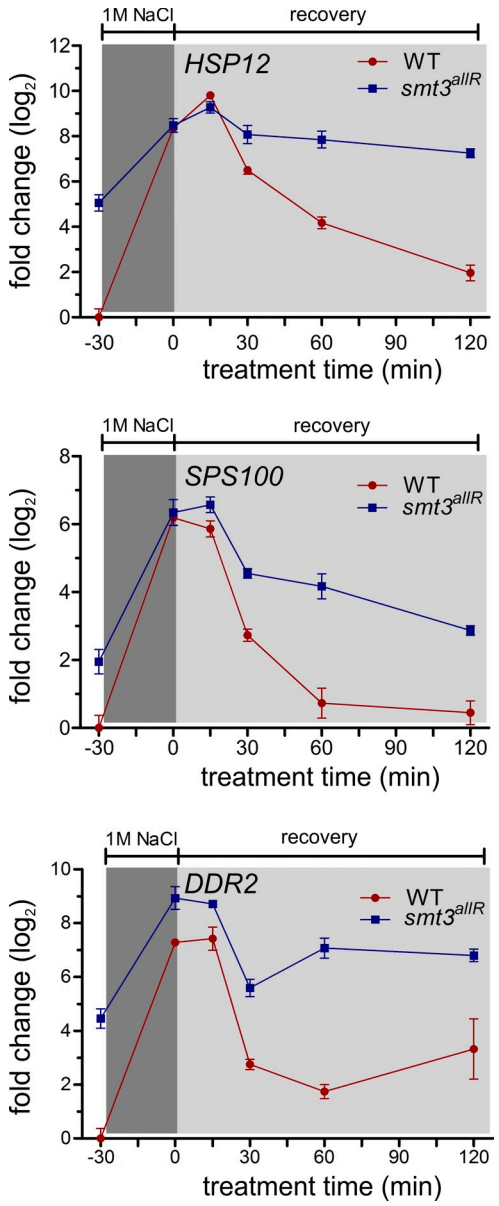

Figure 5. **SUMO chains are required to establish a basal transcription setpoint for stress-regulated genes.** Parental and *smt3*^{allR} strains were grown in YPD and treated with 1 M NaCl for 30 min, then allowed to recover in YPD medium. Aliquots were collected at the indicated time points for RNA preparation. *HSP12*, *SPS100*, and *DDR2* mRNA were monitored by qRT-PCR and values were normalized to *ACT1* levels. Error bars indicate standard deviation from three or more biological replicates

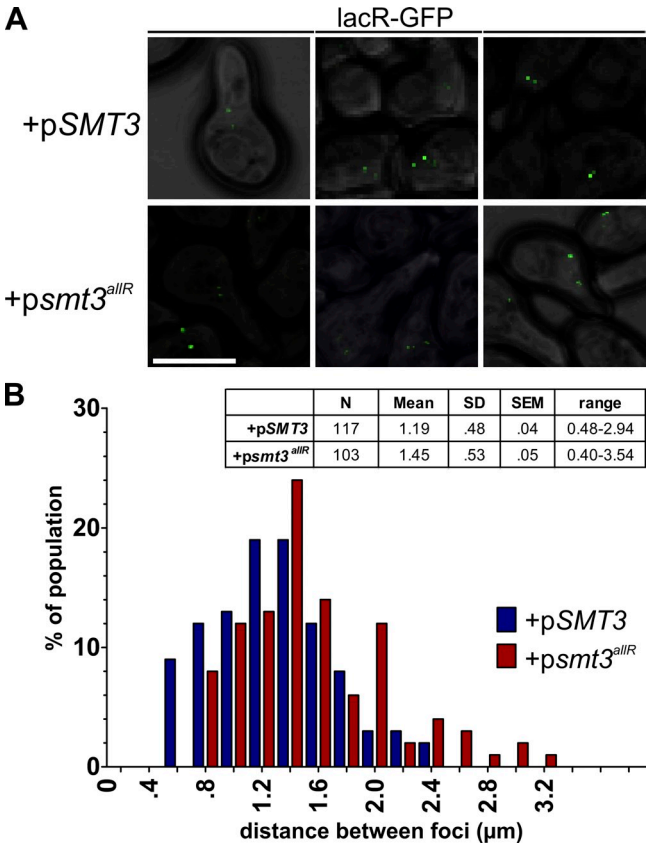

Figure 6. **Higher-order chromatin organization is disrupted in cells expressing the SUMO allR protein.** (A) WT SUMO or smt3^{allR} protein expression was induced in AVY89 (lacO/lacR-GFP) cells for 16 h, and the distance between GFP foci on chromosome IV was measured as in Vas et al. (2007). Bar, 5 µm. (B) Data (from >100 cells) are presented in tabular form (values are expressed in micrometers) and as a bar graph with binned distance values, as indicated. Data shown are from a single representative experiment, conducted twice.

rDNA copy number (Conconi et al., 1989; Dammann et al., 1995). The SUMO system plays an important (but poorly understood) role in these processes (Takahashi et al., 2008; unpublished data). To better understand the role of SUMO chains in rDNA organization and maintenance, several different nucleolar markers were expressed and analyzed in parental and *smt3*^{allR} cells. Notably, the NOP2-GFP protein exhibited a much more diffuse pattern in cycling *smt3*^{allR} cells (Fig. S5 C), implicating SUMO chain function in the organization of nucleolar DNA. To confirm and extend this result, NOP58-GFP–, NOP13-GFP–, and NET1-GFP–expressing cells were arrested in S phase by HU treatment (0.2 M for 90 min) and released into nocodazole-containing medium (15 µg/ml for 90 min) to synchronize them at the G2/M boundary, when budding yeast rDNA is partially compacted in preparation for mitosis (Guacci et al., 1994; D'Ambrosio et al., 2008). The signal volume of NOP58-GFP and NOP13-GFP was much more variable in *smt3*^{allR} cells as compared with parental strains (Fig. 7, B and C). Similarly, although the total NET1-GFP fluorescence signal intensity was equal in both strains, the signal volume was much more variable, and larger on average, in *smt3*^{allR} cells ($P < 0.0001$; Fig. 7, D and E). Together, these data indicate that nucleolar DNA organization is also altered in a budding yeast mutant unable to synthesize SUMO chains.

Previous work has demonstrated that a loss of rDNA repeat organization or localization can lead to changes in rDNA copy number (Takahashi et al., 2008; Chan et al., 2011). Using quantitative PCR (qPCR), we found that the rDNA repeat number is significantly increased in *smt3*^{allR} cells, as compared with their parental counterparts (Fig. 7 F). Similar to chromosome IV and telomeres, rDNA compaction and/or organization (as judged by several different GFP markers and quantitation of rDNA repeat number) is thus also compromised when SUMO chain function is disrupted.

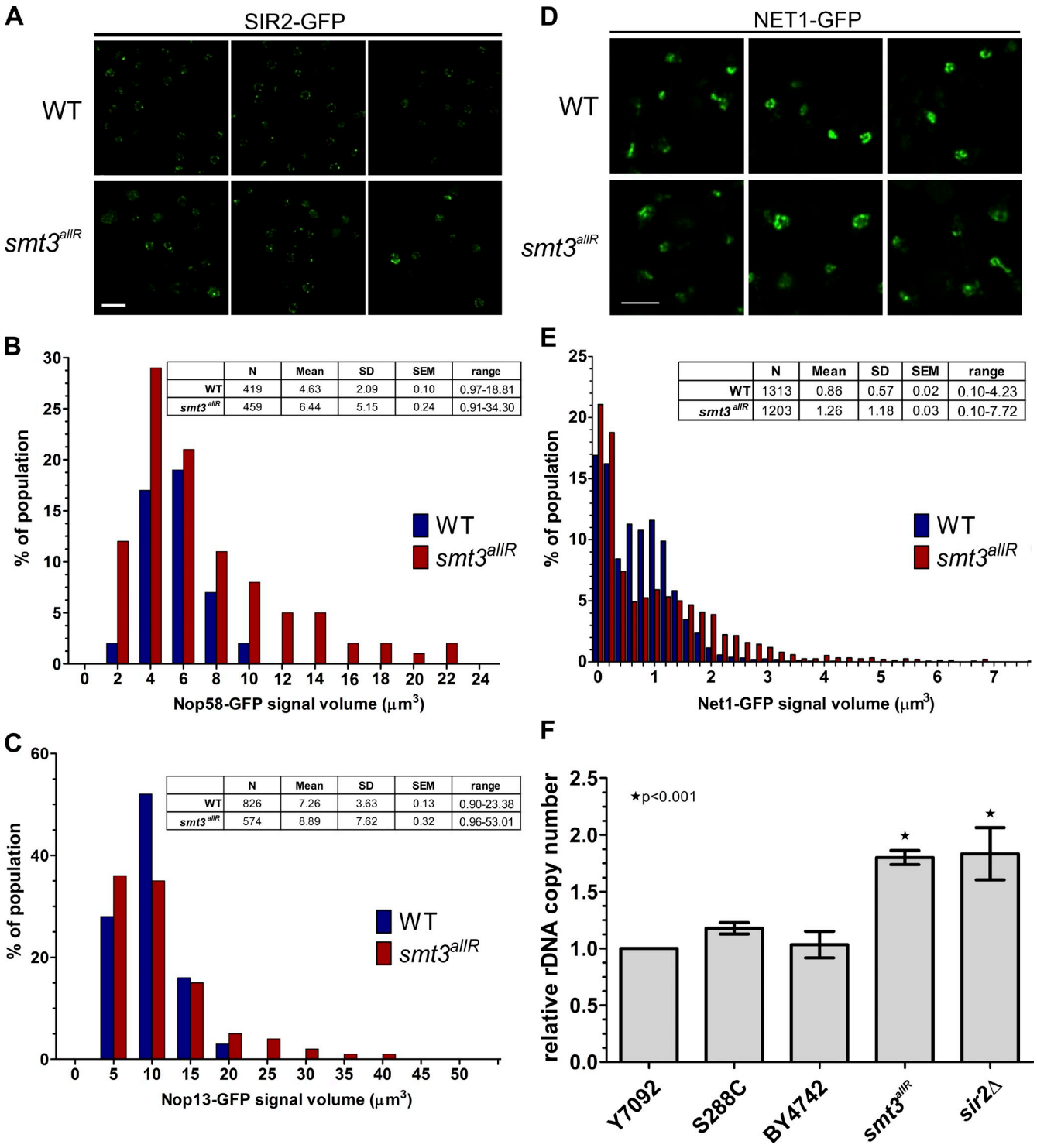

Figure 7. **Nucleolar and telomere organization are disrupted in cells expressing the SUMO allR protein.** (A) SIR2-GFP was imaged in log-phase cells in parental and *smt3*^{allR} backgrounds. (B–E) GFP-tagged NOP58, NOP13, and NET1 strains were arrested in S phase by HU treatment and released into nocodazole-containing medium. Nucleolar/rDNA area was analyzed by quantifying NOP58 (n > 400), NOP13 (n > 500), and NET1 (n > 1,200) GFP signals. Volocity software was used to automate measurements of GFP signal volume across 9 z stacks. (D) Confocal micrographs of NET1-GFP in parental and *smt3*^{allR} cells. Data shown are from a single representative experiment, conducted twice. Bars, 5 μm. (F) rDNA copy number (relative to the WT strain Y7092) was measured by qPCR using the ΔΔCt method. Experiments were performed in triplicate (where each reaction was also performed in triplicate); error bars indicate standard deviation.

Discussion

Many transcription factors, coregulators, and chromatin remodeling proteins are SUMO targets (for review see Gill, 2005), and sumoylation of chromatin remodelers in yeast and mammalian cells has been suggested to be required for the formation of a local heterochromatin-like state on some promoters (Uchimura et al., 2006). A recent study indicated that Ubc9

inactivation in *S. cerevisiae* leads to increased transcription at the inducible *ARG1* gene and impaired the ability of these cells to inactivate *ARG1* transcription after removal of the activation signal (Rosonina et al., 2010). SUMO has also been reported to be enriched in heterochromatic DNA regions (Uchimura et al., 2006), and sumoylation of the ubiquitous transcription factor Sp3 has been linked to local heterochromatinization (Stielow et al., 2008b), whereas expression of an unsumoylatable Sp3 protein leads to derepression of several tissue-specific genes in mammalian cells (Stielow et al., 2010). Here, we find that disruption of SUMO chains in yeast negatively affects higher-order chromatin organization and the maintenance of transcriptional repression. We propose that a general, widespread defect in chromatin packaging (as reflected by increased distances between two chromosomal markers, disorganized telomere clustering, and altered nucleolar rDNA organization) leads to transcriptional derepression throughout the genome. In this way, SUMO chains appear to play an important role in establishing a basal transcription setpoint. Our data also indicate that SUMO chains are not required for stress-regulated transcriptional activation. However, the precise role of SUMO chains in transcriptional inactivation is not yet clear: although SUMO chains are clearly required to maintain transcriptional repression in yeast, they do not seem to be required for at least a partial inactivation of transcription after stress (Fig. 5). Additional exploration of the role of SUMO chains in transcriptional inactivation may shed further light on these findings.

The SUMO system has also been implicated in DNA replication and DNA damage repair (Makhnevych et al., 2009; Cremona et al., 2012). Our data specifically implicate SUMO chains in DNA replication–associated DNA damage. How might this damage occur in *smt3^{allR}* cells? DNA lesions can block the progress of DNA replication forks. Although replication can restart via repriming downstream of the damaged area (Heller and Marians, 2006), the repriming process generates a single-stranded gap near the lesion (Lehmann and Fuchs, 2006). To fill these gaps, the template switch (TS) pathway may be used. TS utilizes undamaged DNA on the sister chromosome via a mechanism that shares similarities with homologous recombination (Goldfless et al., 2006; Branzei and Foiani, 2007). The TS process gives rise to X-shaped DNA intermediates, with biochemical properties similar to pseudodouble Holliday junctions (for review see Klein, 2006). A failure to resolve these structures can lead to DNA damage and chromosomal rearrangements. The RecQ helicase Sgs1 (the budding yeast orthologue of the human BLM protein) is required for resolution of these structures (Liberi et al., 2005; Wu and Hickson, 2006), and the ability of Sgs1 to promote their dissolution is regulated by the SUMO pathway (Branzei et al., 2006). Recent work has also demonstrated that the Smc5-6 complex, Esc2, and the Mms4-Mus81 complex (all of which were detected in our SGA and HCS analyses) play important roles in resolving these recombination intermediates on damaged DNA templates (Branzei et al., 2006; Chavez et al., 2010). Mutant *smc5-6* and *smc6-9* cells are sensitive to MMS treatment, and undergo aberrant mitosis in which chromosome segregation of repetitive regions is impaired (Torres-Rosell et al., 2005). Consistent with these data, the SUMO mutant strain *smt3-331* was isolated in a high-content screen for cells unable to properly segregate GFP-labeled chromosomes (Biggins et al., 2001). Our *smt3^{allR}* mutant shares several similarities with this group of strains, implicating SUMO chains in the same processes.

It is important to note that the SUMO proteins may be regulated by posttranslational modifications such as phosphorylation, acetylation, and ubiquitylation (Matic et al., 2008; Mazur and van den Burg, 2012). However, acetylation of lysine residues in the human SUMO proteins inhibits (or has no effect on) SUMO–SIM interactions, and K-to-R mutations at acetylation sites do not affect their activity in transcriptional repression and protein binding assays (Ullmann et al., 2012). As reported here, the 3KR yeast SUMO mutant has the same effect as the allR SUMO protein in assays of division time, ploidy, and mRNA expression levels. K-to-R mutations are thus not likely to significantly disrupt SUMO function, other than to abrogate chain synthesis. Nevertheless, because we do not completely understand how the yeast SUMO protein may be posttranslationally modified, we cannot rule out this possibility.

Finally, our data also have clear implications for human disease. For example, a SUMO chain deficit could render cells more susceptible to chemotherapeutic agents because of a heavier DNA damage load and increased chromosome missegregation. Indeed, although the molecular details of this phenomenon are not yet understood, a recent study linked SUMO E1 mutations to improved outcome in some (*Myc* mutation–associated) breast cancers (Kessler et al., 2012). Combined with our observations, these data suggest that targeting of the SUMO system (and in particular SUMO chain synthesis) could have therapeutic value.

Materials and methods

Yeast strains and plasmids

S. cerevisiae strains used in this study were derivatives of the BY4741/2 haploid cells, unless otherwise specified, and are listed in Table S4. All yeast genetic manipulations were performed according to established procedures. Unless otherwise noted, yeast strains were grown at 30°C to mid-logarithmic phase in YPD or selective minimal (SM) media supplemented with appropriate nutrients and 2% glucose. Transformations were performed as described previously (Delorme, 1989). The AVY89 strain was kindly provided by D.J. Clarke (University of Minnesota Medical School, Minneapolis, MN).

Construction of *smt3^{allR}* strains

Multistep PCR was used to generate a product containing the NatMX cassette from p4339, 207 bp of the Smt3 5′ UTR from genomic DNA, the *smt3^{allR}* coding DNA sequence from Bylebyl et al. (2003), and 273 bp of the Smt3 3′ UTR from genomic DNA. The resulting product was used to transform yeast strains as in Gietz and Woods (2002). See Table S5 for primers.

Whole cell lysate preparation, affinity purification, SDS-PAGE, and Western blotting

Whole cell lysates were prepared by alkaline lysis and trichloroacetic acid protein precipitation of cell pellets derived from 10-ml cultures. Protein pellets were resuspended in SDS-PAGE sample buffer, sonicated for 10 s, and incubated at 90°C for 5 min before SDS-PAGE. Proteins were transferred to a nitrocellulose membrane (Pall) and probed with HA.11 (Covance), anti-Smt3 (Covance), or anti-actin (EMD Millipore). Proteins were visualized with secondary HRP-conjugated anti–mouse or anti–rabbit antibodies (Bio-Rad Laboratories) and ECL (Immuno-Star HRP; Bio-Rad Laboratories).

Recombinant protein purification and quantification

pGEX-6P-1-SMT3 or pGEX-6P-1-smt3^{allR}, encoding an N-terminal GST moiety fused to the *SMT3* or *smt3^{allR}* coding regions (1–294), was constructed using standard cloning techniques, and verified by DNA sequencing. The

pGEX-6P-1-SUMO proteins were expressed in BL21 *Escherichia coli* induced with 2 mM isopropyl-β-D-1-thiogalactopyranoside at 16°C for 16 h. Proteins were purified using MagneGST glutathione particles (Promega), according to manufacturer's instructions. WT and allR SUMO proteins were cleaved free of the GST moiety using a 4% PreScission Protease solution (GE Healthcare) at 4°C for 16 h. Proteins were assessed for purity using SDS-PAGE and quantified with a Bradford assay. Coomassie-stained SDS-PAGE gels were digitized using a scanner (Epson), and intensity measurements on individual bands were made on the digitized images using Photoshop CS4 (Adobe) software.

In vitro sumoylation

Assays were performed with 150 ng of E1 (AOS1/UBA2), 1 µg of E2 (UBC9), 2 µl of 10× sumoylation reaction buffer (200 mM Hepes, pH 7.5, 50 mM $MgCl_2$, and 20 mM ATP), 1 µg of SUMO, and 250 ng of biotinylated substrate (all proteins from Boston Biochem). The reaction mixture was incubated at 30°C for 2 h, then quenched with SDS-PAGE sample buffer. Reactions were analyzed by SDS-PAGE followed by Western blotting using streptavidin-conjugated HRP (Bio-Rad Laboratories). After transfer to a nitrocellulose membrane (Pall), proteins were visualized using a 2% solution of Ponceau S in 1% acetic acid.

Electron microscopy

Samples were prepared as in Wright (2000), and visualized on a transmission electron microscope (H-7000; Hitachi). In brief, cells were fixed with 4% glutaraldehyde at room temperature for 5 min. Cells were washed and secondary fixed with 2% potassium permanganate at room temperature for 5 min. Cells were then washed and overlayed with 1% uranyl acetate for 1 h at room temperature. Cells were then dehydrated by incubating in increasing amounts of ethanol over an 8-h period. Next, cells were infiltrated in Spurr's resin and samples were polymerized in embedding mold at 60°C for 48 h. 90-nm-thin sections were mounted on 200 mesh copper grids and stained with lead citrate for 5 min before observation with the transmission electron microscope (H7000) at 75 kV. Images were captured in TIF format.

Oxygen consumption rate measurements

Cultures were grown overnight (O/N) in YPD media and diluted in the morning to OD_{600} 0.1 in fresh YPD media. 1 ml of OD_{600} 0.3 culture was collected, washed twice with 50 mM potassium phosphate buffer, pH 6.8, and resuspended to OD_{600} 0.3. Resuspended cells were used to seed XF96 plates (Seahorse Biosciences). Plates were centrifuged at 2,000 rpm for 2 min, then allowed to rest for 30 min at 30°C. The Seahorse sensor cartridge was rehydrated O/N as per the manufacturer's instructions. XF96 culture plates and sensor cartridge were mated and placed in a Seahorse instrument, set to maintain temperature at 30°C. An initial wait time of 20 min was added to allow equilibration of the culture to instrument conditions. After 1 min of mixing, a 1-min wait time was also included to allow for cell settling, before measuring for 2 min. Three measurements were taken for the basal reading, before the addition of azide to a final concentration of 0.05% in media. Three additional readings were then taken. The mean of the three readings across the 2-min span was calculated for each well. Six wells were used for each strain.

High-content microscopic screen

An array consisting of 384 strains (Table S3) from the yeast GFP collection (Huh et al., 2003) expressing proteins previously demonstrated to display altered localization or intensity in response to replication stress (Tkach et al., 2012) was constructed and crossed with the *smt3^{allR}* mutant (*smt3^{allR}::NatMX NUP49-mCherry::URA3 or pro-smt3^{allR}::NatMX NUP49-mCherry::URA3*) using SGA (Tong and Boone, 2007) to yield 384 GFP-ORF strains bearing the *smt3^{allR}* allele. GFP protein localization and relative steady-state abundance for each strain in the WT and *smt3^{allR}* mutants were determined essentially as described in Tkach et al. (2012). In brief, cultures were grown to mid-log phase in low-fluorescence medium and transferred to 384-well slides at a final density of 0.045 OD_{600}/ml. Four images per well in the green and red channels (800 ms exposure) were simultaneously acquired, imaged using a high-throughput confocal microscope system (EVOTEC Opera; PerkinElmer) with quad-band dichroic filter (405/488/561/653). The images were blinded and scored manually for localization and relative abundance changes versus the WT GFP-ORF (Huh et al., 2003). A brief description was recorded for each protein undergoing a change in the *smt3^{allR}* or *pro-smt3^{allR}* strains.

Confocal microscopy

Mid-log phase cells were collected from 1-ml cultures, washed in brief in H_2O containing 2% glucose, and mounted on a glass slide. Cells were imaged at room temperature using a 100×/1.40 NA Plan-Apochromat lens on an inverted microscope (IX80; Olympus) fitted with a spinning disk confocal scanner unit (Yokogawa CSU10; Quorum Technologies, Inc.) and a 512 × 512 EM charge-coupled device (CCD) camera (Hamamatsu Photonics). Diode lasers at 561 nm (RFP), 491 nm (GFP), and 405 nm (DAPI) were used for excitation combined with the following filter sets: 500/20 nm, 430/10 nm, and 555/28 nm. The system was controlled with Volocity 5.5 software (PerkinElmer). The CCD camera was operated at maximum resolution. Exposure times, gain, and sensitivity varied by protein; however, the same settings were used in WT and *smt3^{allR}* strains. Settings were maintained for all subsequent images of the same strain. Cropping and gamma adjustments of images were performed using Volocity (image export) and Photoshop CS4.

For experiments requiring fluorescent labeling of vacuoles, FM4-64 was added to culture media to a concentration of 20 µM and incubated at 30°C for 30 min. Cultures were washed twice with media, then resuspended in fresh media and allowed to grow for another hour before imaging. To achieve hypertonic shock, cells were treated with 0.4 M NaCl for 10 min before imaging. To achieve hypotonic shock, cells were treated with 20 mM MES for 10 min before imaging. Nine z stacks 0.4 µm apart were acquired. Exposure time, sensitivity, gain, laser power, and binning were kept constant between all strains.

For fluorescent mitochondrial labeling, the plasmid pVT100U-mtGFP (Westermann and Neupert, 2000) was transformed into strains using electroporation. Strains were grown O/N, diluted to an OD_{600} of 0.2, and allowed to grow for 3 h. 0.1 µM MitoTracker red CMXRos (Invitrogen) and 7.5 µg/ml DAPI (Biotium, Inc.) were added to the culture media and incubated at 30°C for 2 h. Cells were then washed once with 1 M sorbitol, resuspended in 0.5 ml of 1 M sorbitol with 30 µl of 37% formaldehyde, and left on the benchtop for 5 min with occasional vortexing. Cells were then pelleted and resuspended in 50 mM Tris, pH 7.4, and stored at 4°C until they were imaged. Nine z stacks 0.4 µm apart were acquired. Exposure time, sensitivity, gain, laser power, and binning were kept constant between all strains.

For nucleolar/rDNA condensation experiments, cells were grown O/N in CSM His– media with 2% glucose at 26°C. The next morning, 1 ml of OD_{600} 0.3 cells were collected and resuspended in YPD containing 0.2 M HU for 90 min at 30°C. Cells were washed three times with water and resuspended in YPD containing 15 µg/µl nocodazole for 90 min at 30°C. Cells were then washed once with 1 M sorbitol and resuspended in 0.5 mL of 1 M sorbitol. Formaldehyde was added to 2% (final) and cells were incubated at room temperature for 5 min, with gentle vortexing every 30 s. Cells were then pelleted and resuspended in 50 mM Tris, pH 7.4, and stored at 4°C until they were imaged. Nine z stacks 0.4 µm apart were acquired. Exposure time, sensitivity, gain, laser power, and binning were kept constant between all strains. Volocity software was used to automatically identify cells using brightfield at 8% threshold cutoff (also a cutoff of >2 μm^3). Within objects identified as a cell, the fluorescence intensity in the GFP channel was measured within 2 SD of the mean, and the volume occupied by this fluorescence signal was computed. The Mann-Whitney test was used to compare means of fluorescence volumes. To represent data graphically, volumes were binned and shown as a percentage of the population.

Flow cytometry analysis

Approximately 10^7 mid-log phase cells were resuspended in 70% EtOH for fixation. Flow cytometry analysis was performed with a flow cytometer (FACSCalibur; BD) and CellQuest Pro software (BD). DNA was stained using the fluorescent dye Sytox green (Invitrogen) at a 1:5,000 dilution. Data were analyzed using a free version of Cyflogic (CyFlo Ltd.).

Cellular glycerol levels

To determine total glycerol content, a 1-ml aliquot of YPD grown cells (OD_{600} = 0.6) was collected by centrifugation, washed twice with water, and resuspended in 0.5 ml of 100 mM Tris, pH 7.4. Samples were boiled for 10 min and centrifuged at 16,000 *g* for 15 min (4°C), and 10 µl of the supernatants were assayed for glycerol content. Glycerol concentration was determined colorimetrically with a commercial kit (EnzyChrom Glycerol Assay kit, EGLY-200; BioAssay Systems), according to the manufacturer's instructions.

SGA analysis/SGA correlation analysis

SGA and correlation analyses were conducted as in Baryshnikova et al. (2010) and Costanzo et al. (2010). In brief, *smt3^{allR}* query strains were crossed with 3,885 nonessential deletion mutants to generate double mutants via several selection steps. The fitness of double mutants was evaluated by measuring colony size in an automated fashion (see Baryshnikova et al., 2010 for details). Genetic interaction profile similarities were measured for

all query and array gene pairs by computing Pearson correlation coefficients (PCC) for the complete genetic interaction matrix in Costanzo et al. (2010) and the SGA with the *smt3*^{allR}. SGA was conducted using two different clones of the *smt3*^{allR} mutant (one expressing the pro-SUMO protein and one expressing the mature SUMO polypeptide) in the Y7092 SGA parental strain. Genes identified to be synthetic sick in both screens were considered to be true positives.

Transcriptome analysis

WT and *smt3*^{allR} strains were grown to mid-log phase in YPD media. Samples were centrifuged and snap-frozen. Total RNA and single-stranded cDNA were prepared according to Juneau et al. (2007), except that actinomycin D was added to a final concentration of 6 µg/ml during cDNA synthesis to prevent antisense artifacts (Perocchi et al., 2007). In brief, RNA was extracted with hot phenol from mid-log phase cultures, and total RNA was treated for 10 min at 37°C with RNase-free DNaseI, repurified using the RNeasy Mini kit (QIAGEN) and eluted with 1× Tris-EDTA buffer, pH 8.0. Single-stranded cDNA was synthesized in 200-µl reactions containing 0.25 µg/µl total RNA, 12.5 ng/µl random primers, 12.5 ng/µl oligo(dT)12-18 primer, 15 units/µl SuperScript II (Invitrogen), 1× first strand buffer, 10 mM DTT, 6 ng/µl actinomycin D, and 10 mM dNTP. After cDNA synthesis, RNA was degraded with 1/3 volume of 1 M NaOH incubated for 30 min, and an addition of 1/3 volume of 1 M HCl was used to neutralize the solution before cleanup with the MinElute Reaction Cleanup kit (QIAGEN). cDNA was fragmented with 2.1 units/µl DNaseI and labeled in 50 µl reactions containing 0.3 mM GeneChip DNA labeling reagent, 1× terminal transfer reaction buffer, and 2 µl of terminal deoxynucleotidyl transferase (Promega) for 60 min at 37°C. Labeled cDNA was hybridized to arrays for 16 h at 45°C. Raw data from Affymetrix GCOS software (.CEL format) was analyzed with Affymetrix Tiling Analysis software (TAS; http://www.affymetrix.com/partners_programs/programs/developer/TilingArrayTools/index.affx). Expression levels were mapped to the chromosomal map from the *Saccharomyces* Genome Database and are available for download as supplemental .bar files.

qRT-PCR

Strains were grown O/N, diluted to OD_{600} 0.2, and grown to 0.6. Cultures were shocked with 1 M NaCl for 30 min, then allowed to recover in fresh YPD media for 120 min. 5-ml culture aliquots were collected at the indicated time points and snap-frozen. The MasterPure Yeast RNA Purification kit (Epicenter) was used according to manufacturer's instructions to prepare purified RNA. RNA quality (RIN) was analyzed using an Agilent 2100 Bioanalyzer and RNA quantity was estimated with a spectrophotometer (Nanodrop 1000; Thermo Fisher Scientific). qRT-PCR primers were designed using the cDNA for each desired target with qPCR settings in Primer3Plus (see Table S5; Untergasser et al., 2007). 40 ng of template RNA and 50 nM of each primer were used with the Power SYBR green RNA-to-CT 1-Step kit (Applied Biosystems) in 20-µl reactions, as per the manufacturer's instructions, on a qPCR system (Mx3000P; Stratagene). Act1 was used as a control for ΔΔCt-based relative quantification (Livak and Schmittgen, 2001).

qPCR

Strains were grown O/N in YPD (200 µg/ml +cloNAT or 100 µg/ml +G418 for mutants), diluted in the morning to OD_{600} of 0.2. Cultures were grown to OD_{600} 0.8, and 10-ml aliquots were snap-frozen. A MasterPure Yeast DNA Purification kit (Epicentre) was used to isolate genomic DNA according to the manufacturer's instructions. Samples were incubated with DNase-free RNase for 2 h in TE before storing at −20°C. DNA was quantified with a spectrophotometer (Nanodrop 1000). A Power Sybr green PCR kit was used in 20-µl reactions containing 1 ng of DNA and 50 nM of each primer, as per the manufacturer's instructions, on a qPCR system (Mx3000P). Primers were as follows: rDNA-F, 5′-TACTGCGAAAGCATTTGCCAAGGACG-3′; rDNA-R, 5′-TCCCCCCAGAACCCAAAGACTTTGAT-3′; act1-F, 5′-CTTTCAACGTTCCAGCCTTC-3′; and act1-R, 5′-CCAGCGTAAATTGGAACGAC-3′.

Online supplemental material

Fig. S1 shows data indicating that the *smt3*^{allR} strains exhibit markedly increased chromosome segregation defects, and additional spot assays. Fig. S2 contains representative images from the HCS showing mislocalized spindle proteins, and highlights characteristics of an environmental stress response in SUMO mutant strains. Fig. S3 contains additional EM images, as well as measurements on internal glycerol content and FM4-64 vacuole-stained images. Fig. S4 contains doubling time, FACS, and gene expression data for strains overexpressing an *smt3*^{3KR} protein. Fig. S5 displays a summarized image of microarray data for the *smt3*^{allR} strain, an expression profile for the Gre1 mRNA during stress response, and representative images from the HCS for NOP2-GFP. Table S1 contains localization and intensity data from the HCS, as well as GO analysis. Table S2 contains all SGA and correlation analysis data, as well as GO analysis. Table S3 contains expression data for all ORFs and known CUTs. Table S4 contains details on strains used in this study. Table S5 lists the sequences of all primers used in this study. Two .bar files, containing expression level changes mapped to chromosome location, are available for download. Online supplemental material is available at http://www.jcb.org/cgi/content/full/jcb.201210019/DC1. Additional data are available in the JCB DataViewer at http://dx.doi.org/10.1083/jcb.201210019.dv.

We thank Yan Chen and Dr. Paul Fraser at the University of Toronto EM facility and Connie Danielsen for expert technical assistance, as well as A.-C. Gingras and the Raught laboratory for critical reading of the manuscript. We are also very grateful to D.J. Clarke for yeast strains.

T. Srikumar was funded by a Canadian Institutes of Health Research student fellowship. Work in the G.W. Brown laboratory was supported by grant 020254 from the Canadian Cancer Society Research Institute. C. Boone and B.J. Andrews were supported by a grant from the National Institutes of Health (1R01HG005853-01) and by grants from the Canadian Institutes of Health Research (MOP-102629 and MOP-97939) and the Ontario Research Fund (GL2-01-22). B. Raught holds the Canada Research Chair in Proteomics and Molecular Medicine, and funding for work in the B. Raught laboratory was provided by Canadian Institutes of Health Research grant MOP81268.

Submitted: 3 October 2012
Accepted: 7 March 2013

References

Abed, M., K.C. Barry, D. Kenyagin, B. Koltun, T.M. Phippen, J.J. Delrow, S.M. Parkhurst, and A. Orian. 2011. Degringolade, a SUMO-targeted ubiquitin ligase, inhibits Hairy/Groucho-mediated repression. *EMBO J.* 30:1289–1301. http://dx.doi.org/10.1038/emboj.2011.42

Ashton, T.M., and I.D. Hickson. 2010. Yeast as a model system to study RecQ helicase function. *DNA Repair (Amst.).* 9:303–314. http://dx.doi.org/10.1016/j.dnarep.2009.12.007

Baryshnikova, A., M. Costanzo, Y. Kim, H. Ding, J. Koh, K. Toufighi, J.Y. Youn, J. Ou, B.J. San Luis, S. Bandyopadhyay, et al. 2010. Quantitative analysis of fitness and genetic interactions in yeast on a genome scale. *Nat. Methods.* 7:1017–1024. http://dx.doi.org/10.1038/nmeth.1534

Bencsath, K.P., M.S. Podgorski, V.R. Pagala, C.A. Slaughter, and B.A. Schulman. 2002. Identification of a multifunctional binding site on Ubc9p required for Smt3p conjugation. *J. Biol. Chem.* 277:47938–47945. http://dx.doi.org/10.1074/jbc.M207442200

Biggins, S., N. Bhalla, A. Chang, D.L. Smith, and A.W. Murray. 2001. Genes involved in sister chromatid separation and segregation in the budding yeast *Saccharomyces cerevisiae*. *Genetics.* 159:453–470.

Branzei, D., and M. Foiani. 2007. Template switching: from replication fork repair to genome rearrangements. *Cell.* 131:1228–1230. http://dx.doi.org/10.1016/j.cell.2007.12.007

Branzei, D., J. Sollier, G. Liberi, X. Zhao, D. Maeda, M. Seki, T. Enomoto, K. Ohta, and M. Foiani. 2006. Ubc9- and mms21-mediated sumoylation counteracts recombinogenic events at damaged replication forks. *Cell.* 127:509–522. http://dx.doi.org/10.1016/j.cell.2006.08.050

Bruderer, R., M.H. Tatham, A. Plechanovova, I. Matic, A.K. Garg, and R.T. Hay. 2011. Purification and identification of endogenous poly-SUMO conjugates. *EMBO Rep.* 12:142–148. http://dx.doi.org/10.1038/embor.2010.206

Bylebyl, G.R., I. Belichenko, and E.S. Johnson. 2003. The SUMO isopeptidase Ulp2 prevents accumulation of SUMO chains in yeast. *J. Biol. Chem.* 278:44113–44120. http://dx.doi.org/10.1074/jbc.M308357200

Castro, P.H., R.M. Tavares, E.R. Bejarano, and H. Azevedo. 2012. SUMO, a heavyweight player in plant abiotic stress responses. *Cell. Mol. Life Sci.* 69:3269–3283. http://dx.doi.org/10.1007/s00018-012-1094-2

Chan, J.N., B.P. Poon, J. Salvi, J.B. Olsen, A. Emili, and K. Mekhail. 2011. Perinuclear cohibin complexes maintain replicative life span via roles at distinct silent chromatin domains. *Dev. Cell.* 20:867–879. http://dx.doi.org/10.1016/j.devcel.2011.05.014

Chavez, A., V. George, V. Agrawal, and F.B. Johnson. 2010. Sumoylation and the structural maintenance of chromosomes (Smc) 5/6 complex slow senescence through recombination intermediate resolution. *J. Biol. Chem.* 285:11922–11930. http://dx.doi.org/10.1074/jbc.M109.041277

Chen, X.L., H.R. Silver, L. Xiong, I. Belichenko, C. Adegite, and E.S. Johnson. 2007. Topoisomerase I-dependent viability loss in *saccharomyces cerevisiae* mutants defective in both SUMO conjugation and DNA repair. *Genetics.* 177:17–30. http://dx.doi.org/10.1534/genetics.107.074708

Conconi, A., R.M. Widmer, T. Koller, and J.M. Sogo. 1989. Two different chromatin structures coexist in ribosomal RNA genes throughout the cell cycle. *Cell*. 57:753–761. http://dx.doi.org/10.1016/0092-8674(89)90790-3

Costanzo, M., A. Baryshnikova, J. Bellay, Y. Kim, E.D. Spear, C.S. Sevier, H. Ding, J.L. Koh, K. Toufighi, S. Mostafavi, et al. 2010. The genetic landscape of a cell. *Science*. 327:425–431. http://dx.doi.org/10.1126/science.1180823

Cremona, C.A., P. Sarangi, Y. Yang, L.E. Hang, S. Rahman, and X. Zhao. 2012. Extensive DNA damage-induced sumoylation contributes to replication and repair and acts in addition to the mec1 checkpoint. *Mol. Cell*. 45:422–432. http://dx.doi.org/10.1016/j.molcel.2011.11.028

D'Ambrosio, C., C.K. Schmidt, Y. Katou, G. Kelly, T. Itoh, K. Shirahige, and F. Uhlmann. 2008. Identification of cis-acting sites for condensin loading onto budding yeast chromosomes. *Genes Dev.* 22:2215–2227. http://dx.doi.org/10.1101/gad.1675708

Dammann, R., R. Lucchini, T. Koller, and J.M. Sogo. 1995. Transcription in the yeast rRNA gene locus: distribution of the active gene copies and chromatin structure of their flanking regulatory sequences. *Mol. Cell. Biol.* 15:5294–5303.

Delorme, E. 1989. Transformation of *Saccharomyces cerevisiae* by electroporation. *Appl. Environ. Microbiol.* 55:2242–2246.

Denison, C., A.D. Rudner, S.A. Gerber, C.E. Bakalarski, D. Moazed, and S.P. Gygi. 2005. A proteomic strategy for gaining insights into protein sumoylation in yeast. *Mol. Cell. Proteomics*. 4:246–254. http://dx.doi.org/10.1074/mcp.M400154-MCP200

Elrouby, N., and G. Coupland. 2010. Proteome-wide screens for small ubiquitin-like modifier (SUMO) substrates identify *Arabidopsis* proteins implicated in diverse biological processes. *Proc. Natl. Acad. Sci. USA*. 107:17415–17420. http://dx.doi.org/10.1073/pnas.1005452107

Felberbaum, R., and M. Hochstrasser. 2008. Ulp2 and the DNA damage response: desumoylation enables safe passage through mitosis. *Cell Cycle*. 7:52–56. http://dx.doi.org/10.4161/cc.7.1.5218

Ferreira, H.C., B. Luke, H. Schober, V. Kalck, J. Lingner, and S.M. Gasser. 2011. The PIAS homologue Siz2 regulates perinuclear telomere position and telomerase activity in budding yeast. *Nat. Cell Biol.* 13:867–874. http://dx.doi.org/10.1038/ncb2263

Fryrear, K.A., X. Guo, O. Kerscher, and O.J. Semmes. 2012. The Sumo-targeted ubiquitin ligase RNF4 regulates the localization and function of the HTLV-1 oncoprotein Tax. *Blood*. 119:1173–1181. http://dx.doi.org/10.1182/blood-2011-06-358564

Galanty, Y., R. Belotserkovskaya, J. Coates, and S.P. Jackson. 2012. RNF4, a SUMO-targeted ubiquitin E3 ligase, promotes DNA double-strand break repair. *Genes Dev.* 26:1179–1195. http://dx.doi.org/10.1101/gad.188284.112

Garcia-Dominguez, M., and J.C. Reyes. 2009. SUMO association with repressor complexes, emerging routes for transcriptional control. *Biochim. Biophys. Acta.* 1789:451–459. http://dx.doi.org/10.1016/j.bbagrm.2009.07.001

Gasch, A.P., P.T. Spellman, C.M. Kao, O. Carmel-Harel, M.B. Eisen, G. Storz, D. Botstein, and P.O. Brown. 2000. Genomic expression programs in the response of yeast cells to environmental changes. *Mol. Biol. Cell*. 11:4241–4257.

Gietz, R.D., and R.A. Woods. 2002. Transformation of yeast by lithium acetate/single-stranded carrier DNA/polyethylene glycol method. *Methods Enzymol.* 350:87–96. http://dx.doi.org/10.1016/S0076-6879(02)50957-5

Gill, G. 2005. Something about SUMO inhibits transcription. *Curr. Opin. Genet. Dev.* 15:536–541. http://dx.doi.org/10.1016/j.gde.2005.07.004

Goldfless, S.J., A.S. Morag, K.A. Belisle, V.A. Sutera Jr., and S.T. Lovett. 2006. DNA repeat rearrangements mediated by DnaK-dependent replication fork repair. *Mol. Cell*. 21:595–604. http://dx.doi.org/10.1016/j.molcel.2006.01.025

Golovnin, A., I. Volkov, and P. Georgiev. 2012. SUMO conjugation is required for the assembly of *Drosophila* Su(Hw) and Mod(mdg4) into insulator bodies that facilitate insulator complex formation. *J. Cell Sci.* 125:2064–2074. http://dx.doi.org/10.1242/jcs.100172

Guacci, V., E. Hogan, and D. Koshland. 1994. Chromosome condensation and sister chromatid pairing in budding yeast. *J. Cell Biol.* 125:517–530. http://dx.doi.org/10.1083/jcb.125.3.517

Hay, R.T. 2005. SUMO: a history of modification. *Mol. Cell*. 18:1–12. http://dx.doi.org/10.1016/j.molcel.2005.03.012

Heller, R.C., and K.J. Marians. 2006. Replication fork reactivation downstream of a blocked nascent leading strand. *Nature*. 439:557–562. http://dx.doi.org/10.1038/nature04329

Hickson, I.D., and H.W. Mankouri. 2011. Processing of homologous recombination repair intermediates by the Sgs1-Top3-Rmi1 and Mus81-Mms4 complexes. *Cell Cycle*. 10:3078–3085. http://dx.doi.org/10.4161/cc.10.18.16919

Hochstrasser, M. 2000. Biochemistry. All in the ubiquitin family. *Science*. 289:563–564. http://dx.doi.org/10.1126/science.289.5479.563

Hohmann, S. 2009. Control of high osmolarity signalling in the yeast *Saccharomyces cerevisiae. FEBS Lett.* 583:4025–4029. http://dx.doi.org/10.1016/j.febslet.2009.10.069

Huh, W.K., J.V. Falvo, L.C. Gerke, A.S. Carroll, R.W. Howson, J.S. Weissman, and E.K. O'Shea. 2003. Global analysis of protein localization in budding yeast. *Nature*. 425:686–691. http://dx.doi.org/10.1038/nature02026

Ivanov, A.V., H. Peng, V. Yurchenko, K.L. Yap, D.G. Negorev, D.C. Schultz, E. Psulkowski, W.J. Fredericks, D.E. White, G.G. Maul, et al. 2007. PHD domain-mediated E3 ligase activity directs intramolecular sumoylation of an adjacent bromodomain required for gene silencing. *Mol. Cell*. 28:823–837. http://dx.doi.org/10.1016/j.molcel.2007.11.012

Jeram, S.M., T. Srikumar, X.D. Zhang, H. Anne Eisenhauer, R. Rogers, P.G. Pedrioli, M. Matunis, and B. Raught. 2010. An improved SUMmOn-based methodology for the identification of ubiquitin and ubiquitin-like protein conjugation sites identifies novel ubiquitin-like protein chain linkages. *Proteomics*. 10:254–265. http://dx.doi.org/10.1002/pmic.200900648

Johnson, E.S. 2004. Protein modification by SUMO. *Annu. Rev. Biochem.* 73:355–382. http://dx.doi.org/10.1146/annurev.biochem.73.011303.074118

Johzuka, K., and T. Horiuchi. 2009. The cis element and factors required for condensin recruitment to chromosomes. *Mol. Cell*. 34:26–35. http://dx.doi.org/10.1016/j.molcel.2009.02.021

Jorgensen, P., J.L. Nishikawa, B.J. Breitkreutz, and M. Tyers. 2002. Systematic identification of pathways that couple cell growth and division in yeast. *Science*. 297:395–400. http://dx.doi.org/10.1126/science.1070850

Juneau, K., C. Palm, M. Miranda, and R.W. Davis. 2007. High-density yeast-tiling array reveals previously undiscovered introns and extensive regulation of meiotic splicing. *Proc. Natl. Acad. Sci. USA*. 104:1522–1527. http://dx.doi.org/10.1073/pnas.0610354104

Kerscher, O., R. Felberbaum, and M. Hochstrasser. 2006. Modification of proteins by ubiquitin and ubiquitin-like proteins. *Annu. Rev. Cell Dev. Biol.* 22:159–180. http://dx.doi.org/10.1146/annurev.cellbio.22.010605.093503

Kessler, J.D., K.T. Kahle, T. Sun, K.L. Meerbrey, M.R. Schlabach, E.M. Schmitt, S.O. Skinner, Q. Xu, M.Z. Li, Z.C. Hartman, et al. 2012. A SUMOylation-dependent transcriptional subprogram is required for Myc-driven tumorigenesis. *Science*. 335:348–353. http://dx.doi.org/10.1126/science.1212728

Klein, H.L. 2006. A SUMOry of DNA replication: synthesis, damage, and repair. *Cell*. 127:455–457. http://dx.doi.org/10.1016/j.cell.2006.10.019

Koh, J.L., H. Ding, M. Costanzo, A. Baryshnikova, K. Toufighi, G.D. Bader, C.L. Myers, B.J. Andrews, and C. Boone. 2010. DRYGIN: a database of quantitative genetic interaction networks in yeast. *Nucleic Acids Res.* 38(Database issue):D502–D507. http://dx.doi.org/10.1093/nar/gkp820

Lallemand-Breitenbach, V., M. Jeanne, S. Benhenda, R. Nasr, M. Lei, L. Peres, J. Zhou, J. Zhu, B. Raught, and H. de Thé. 2008. Arsenic degrades PML or PML-RARalpha through a SUMO-triggered RNF4/ubiquitin-mediated pathway. *Nat. Cell Biol.* 10:547–555. http://dx.doi.org/10.1038/ncb1717

Lee, M.T., A.A. Bakir, K.N. Nguyen, and J. Bachant. 2011. The SUMO isopeptidase Ulp2p is required to prevent recombination-induced chromosome segregation lethality following DNA replication stress. *PLoS Genet.* 7:e1001355. http://dx.doi.org/10.1371/journal.pgen.1001355

Lehmann, A.R., and R.P. Fuchs. 2006. Gaps and forks in DNA replication: Rediscovering old models. *DNA Repair (Amst.)*. 5:1495–1498. http://dx.doi.org/10.1016/j.dnarep.2006.07.002

Li, S.J., and M. Hochstrasser. 1999. A new protease required for cell-cycle progression in yeast. *Nature*. 398:246–251. http://dx.doi.org/10.1038/18457

Li, Y.J., J.M. Stark, D.J. Chen, D.K. Ann, and Y. Chen. 2010. Role of SUMO: SIM-mediated protein-protein interaction in non-homologous end joining. *Oncogene*. 29:3509–3518. http://dx.doi.org/10.1038/onc.2010.108

Liberi, G., G. Maffioletti, C. Lucca, I. Chiolo, A. Baryshnikova, C. Cotta-Ramusino, M. Lopes, A. Pellicioli, J.E. Haber, and M. Foiani. 2005. Rad51-dependent DNA structures accumulate at damaged replication forks in sgs1 mutants defective in the yeast ortholog of BLM RecQ helicase. *Genes Dev.* 19:339–350. http://dx.doi.org/10.1101/gad.322605

Linger, J., and J.K. Tyler. 2005. The yeast histone chaperone chromatin assembly factor 1 protects against double-strand DNA-damaging agents. *Genetics*. 171:1513–1522. http://dx.doi.org/10.1534/genetics.105.043000

Livak, K.J., and T.D. Schmittgen. 2001. Analysis of relative gene expression data using real-time quantitative PCR and the 2(-Delta Delta C(T)) Method. *Methods*. 25:402–408. http://dx.doi.org/10.1006/meth.2001.1262

MacPherson, M.J., L.G. Beatty, W. Zhou, M. Du, and P.D. Sadowski. 2009. The CTCF insulator protein is posttranslationally modified by SUMO. *Mol. Cell. Biol.* 29:714–725. http://dx.doi.org/10.1128/MCB.00825-08

Makhnevych, T., C. Ptak, C.P. Lusk, J.D. Aitchison, and R.W. Wozniak. 2007. The role of karyopherins in the regulated sumoylation of septins. *J. Cell Biol.* 177:39–49. http://dx.doi.org/10.1083/jcb.200608066

Makhnevych, T., Y. Sydorskyy, X. Xin, T. Srikumar, F.J. Vizeacoumar, S.M. Jeram, Z. Li, S. Bahr, B.J. Andrews, C. Boone, and B. Raught. 2009. Global map of SUMO function revealed by protein-protein interaction and genetic networks. *Mol. Cell*. 33:124–135. http://dx.doi.org/10.1016/j.molcel.2008.12.025

Matic, I., B. Macek, M. Hilger, T.C. Walther, and M. Mann. 2008. Phosphorylation of SUMO-1 occurs in vivo and is conserved through evolution. *J. Proteome Res.* 7:4050–4057. http://dx.doi.org/10.1021/pr800368m

Mazur, M.J., and H.A. van den Burg. 2012. Global SUMO proteome responses guide gene regulation, mRNA biogenesis, and plant stress responses. *Front Plant Sci*. 3:215. http://dx.doi.org/10.3389/fpls.2012.00215

Mekhail, K., J. Seebacher, S.P. Gygi, and D. Moazed. 2008. Role for perinuclear chromosome tethering in maintenance of genome stability. *Nature*. 456:667–670. http://dx.doi.org/10.1038/nature07460

Meluh, P.B., and D. Koshland. 1995. Evidence that the MIF2 gene of *Saccharomyces cerevisiae* encodes a centromere protein with homology to the mammalian centromere protein CENP-C. *Mol. Biol. Cell*. 6:793–807.

Nathan, D., K. Ingvarsdottir, D.E. Sterner, G.R. Bylebyl, M. Dokmanovic, J.A. Dorsey, K.A. Whelan, M. Krsmanovic, W.S. Lane, P.B. Meluh, et al. 2006. Histone sumoylation is a negative regulator in *Saccharomyces cerevisiae* and shows dynamic interplay with positive-acting histone modifications. *Genes Dev.* 20:966–976. http://dx.doi.org/10.1101/gad.1404206

Nie, M., Y. Xie, J.A. Loo, and A.J. Courey. 2009. Genetic and proteomic evidence for roles of *Drosophila* SUMO in cell cycle control, Ras signaling, and early pattern formation. *PLoS ONE*. 4:e5905. http://dx.doi.org/10.1371/journal.pone.0005905

Nie, M., A. Aslanian, J. Prudden, J. Heideker, A.A. Vashisht, J.A. Wohlschlegel, J.R. Yates III, and M.N. Boddy. 2012. Dual recruitment of Cdc48 (p97)-Ufd1-Npl4 ubiquitin-selective segregase by small ubiquitin-like modifier protein (SUMO) and ubiquitin in SUMO-targeted ubiquitin ligase-mediated genome stability functions. *J. Biol. Chem.* 287:29610–29619. http://dx.doi.org/10.1074/jbc.M112.379768

Ouyang, J., Y. Shi, A. Valin, Y. Xuan, and G. Gill. 2009. Direct binding of CoREST1 to SUMO-2/3 contributes to gene-specific repression by the LSD1/CoREST1/HDAC complex. *Mol. Cell*. 34:145–154. http://dx.doi.org/10.1016/j.molcel.2009.03.013

Panse, V.G., B. Küster, T. Gerstberger, and E. Hurt. 2003. Unconventional tethering of Ulp1 to the transport channel of the nuclear pore complex by karyopherins. *Nat. Cell Biol.* 5:21–27. http://dx.doi.org/10.1038/ncb893

Pérez de Castro, I., C. Aguirre-Portolés, B. Martin, G. Fernández-Miranda, A. Klotzbucher, M.H. Kubbutat, D. Megías, Y. Arlot-Bonnemains, and M. Malumbres. 2011. A SUMOylation motif in Aurora-A: implications for spindle dynamics and oncogenesis. *Front Oncol*. 1:50.

Perocchi, F., Z. Xu, S. Clauder-Münster, and L.M. Steinmetz. 2007. Antisense artifacts in transcriptome microarray experiments are resolved by actinomycin D. *Nucleic Acids Res.* 35:e128. http://dx.doi.org/10.1093/nar/gkm683

Perry, J.J., J.A. Tainer, and M.N. Boddy. 2008. A SIM-ultaneous role for SUMO and ubiquitin. *Trends Biochem. Sci.* 33:201–208. http://dx.doi.org/10.1016/j.tibs.2008.02.001

Prudden, J., S. Pebernard, G. Raffa, D.A. Slavin, J.J. Perry, J.A. Tainer, C.H. McGowan, and M.N. Boddy. 2007. SUMO-targeted ubiquitin ligases in genome stability. *EMBO J.* 26:4089–4101. http://dx.doi.org/10.1038/sj.emboj.7601838

Rand, J.D., and C.M. Grant. 2006. The thioredoxin system protects ribosomes against stress-induced aggregation. *Mol. Biol. Cell*. 17:387–401. http://dx.doi.org/10.1091/mbc.E05-06-0520

Rosonina, E., S.M. Duncan, and J.L. Manley. 2010. SUMO functions in constitutive transcription and during activation of inducible genes in yeast. *Genes Dev.* 24:1242–1252. http://dx.doi.org/10.1101/gad.1917910

Ross, S., J.L. Best, L.I. Zon, and G. Gill. 2002. SUMO-1 modification represses Sp3 transcriptional activation and modulates its subnuclear localization. *Mol. Cell*. 10:831–842. http://dx.doi.org/10.1016/S1097-2765(02)00682-2

Rossi, M.L., A.K. Ghosh, and V.A. Bohr. 2010. Roles of Werner syndrome protein in protection of genome integrity. *DNA Repair (Amst.)*. 9:331–344. http://dx.doi.org/10.1016/j.dnarep.2009.12.011

Ryan, M., L.A. Graham, and T.H. Stevens. 2008. Voa1p functions in V-ATPase assembly in the yeast endoplasmic reticulum. *Mol. Biol. Cell*. 19:5131–5142. http://dx.doi.org/10.1091/mbc.E08-06-0629

Saether, T., D.R. Pattabiraman, A.H. Alm-Kristiansen, L.T. Vogt-Kielland, T.J. Gonda, and O.S. Gabrielsen. 2011. A functional SUMO-interacting motif in the transactivation domain of c-Myb regulates its myeloid transforming ability. *Oncogene*. 30:212–222. http://dx.doi.org/10.1038/onc.2010.397

Santiago, A., A.C. Godsey, J. Hossain, L.Y. Zhao, and D. Liao. 2009. Identification of two independent SUMO-interacting motifs in Daxx: evolutionary conservation from *Drosophila* to humans and their biochemical functions. *Cell Cycle*. 8:76–87. http://dx.doi.org/10.4161/cc.8.1.7493

Schwartz, D.C., R. Felberbaum, and M. Hochstrasser. 2007. The Ulp2 SUMO protease is required for cell division following termination of the DNA damage checkpoint. *Mol. Cell. Biol.* 27:6948–6961. http://dx.doi.org/10.1128/MCB.00774-07

Seufert, W., B. Futcher, and S. Jentsch. 1995. Role of a ubiquitin-conjugating enzyme in degradation of S- and M-phase cyclins. *Nature*. 373:78–81. http://dx.doi.org/10.1038/373078a0

Shiio, Y., and R.N. Eisenman. 2003. Histone sumoylation is associated with transcriptional repression. *Proc. Natl. Acad. Sci. USA*. 100:13225–13230. http://dx.doi.org/10.1073/pnas.1735528100

Shin, E.J., H.M. Shin, E. Nam, W.S. Kim, J.H. Kim, B.H. Oh, and Y. Yun. 2012. DeSUMOylating isopeptidase: a second class of SUMO protease. *EMBO Rep.* 13:339–346. http://dx.doi.org/10.1038/embor.2012.3

Stielow, B., A. Sapetschnig, I. Krüger, N. Kunert, A. Brehm, M. Boutros, and G. Suske. 2008a. Identification of SUMO-dependent chromatin-associated transcriptional repression components by a genome-wide RNAi screen. *Mol. Cell*. 29:742–754. http://dx.doi.org/10.1016/j.molcel.2007.12.032

Stielow, B., A. Sapetschnig, C. Wink, I. Krüger, and G. Suske. 2008b. SUMO-modified Sp3 represses transcription by provoking local heterochromatic gene silencing. *EMBO Rep.* 9:899–906. http://dx.doi.org/10.1038/embor.2008.127

Stielow, B., I. Krüger, R. Diezko, F. Finkernagel, N. Gillemans, J. Kong-a-San, S. Philipsen, and G. Suske. 2010. Epigenetic silencing of spermatocyte-specific and neuronal genes by SUMO modification of the transcription factor Sp3. *PLoS Genet.* 6:e1001203. http://dx.doi.org/10.1371/journal.pgen.1001203

Sun, H., J.D. Leverson, and T. Hunter. 2007. Conserved function of RNF4 family proteins in eukaryotes: targeting a ubiquitin ligase to SUMOylated proteins. *EMBO J.* 26:4102–4112. http://dx.doi.org/10.1038/sj.emboj.7601839

Takahashi, Y., M. Iwase, M. Konishi, M. Tanaka, A. Toh-e, and Y. Kikuchi. 1999. Smt3, a SUMO-1 homolog, is conjugated to Cdc3, a component of septin rings at the mother-bud neck in budding yeast. *Biochem. Biophys. Res. Commun.* 259:582–587. http://dx.doi.org/10.1006/bbrc.1999.0821

Takahashi, Y., S. Dulev, X. Liu, N.J. Hiller, X. Zhao, and A. Strunnikov. 2008. Cooperation of sumoylated chromosomal proteins in rDNA maintenance. *PLoS Genet.* 4:e1000215. http://dx.doi.org/10.1371/journal.pgen.1000215

Tang, H.M., K.L. Siu, C.M. Wong, and D.Y. Jin. 2009. Loss of yeast peroxiredoxin Tsa1p induces genome instability through activation of the DNA damage checkpoint and elevation of dNTP levels. *PLoS Genet.* 5:e1000697. http://dx.doi.org/10.1371/journal.pgen.1000697

Tatham, M.H., M.C. Geoffroy, L. Shen, A. Plechanovova, N. Hattersley, E.G. Jaffray, J.J. Palvimo, and R.T. Hay. 2008. RNF4 is a poly-SUMO-specific E3 ubiquitin ligase required for arsenic-induced PML degradation. *Nat. Cell Biol.* 10:538–546. http://dx.doi.org/10.1038/ncb1716

Tempé, D., M. Piechaczyk, and G. Bossis. 2008. SUMO under stress. *Biochem. Soc. Trans.* 36:874–878. http://dx.doi.org/10.1042/BST0360874

Tkach, J.M., A. Yimit, A.Y. Lee, M. Riffle, M. Costanzo, D. Jaschob, J.A. Hendry, J. Ou, J. Moffat, C. Boone, et al. 2012. Dissecting DNA damage response pathways by analysing protein localization and abundance changes during DNA replication stress. *Nat. Cell Biol.* 14:966–976. http://dx.doi.org/10.1038/ncb2549

Tong, A.H.Y., and C. Boone. 2007. High-throughput strain construction and systematic synthetic lethal screening in *Saccharomyces cerevisiae*. *In* Yeast Gene Analysis, Second Edition. 36:369–707.

Torres-Rosell, J., F. Machín, S. Farmer, A. Jarmuz, T. Eydmann, J.Z. Dalgaard, and L. Aragón. 2005. SMC5 and SMC6 genes are required for the segregation of repetitive chromosome regions. *Nat. Cell Biol.* 7:412–419. http://dx.doi.org/10.1038/ncb1239

Tsui, K., T. Durbic, M. Gebbia, and C. Nislow. 2012. Genomic approaches for determining nucleosome occupancy in yeast. *Methods Mol. Biol.* 833:389–411. http://dx.doi.org/10.1007/978-1-61779-477-3_23

Uchimura, Y., T. Ichimura, J. Uwada, T. Tachibana, S. Sugahara, M. Nakao, and H. Saitoh. 2006. Involvement of SUMO modification in MBD1- and MCAF1-mediated heterochromatin formation. *J. Biol. Chem.* 281:23180–23190. http://dx.doi.org/10.1074/jbc.M602280200

Ullmann, R., C.D. Chien, M.L. Avantaggiati, and S. Muller. 2012. An acetylation switch regulates SUMO-dependent protein interaction networks. *Mol. Cell*. 46:759–770. http://dx.doi.org/10.1016/j.molcel.2012.04.006

Untergasser, A., H. Nijveen, X. Rao, T. Bisseling, R. Geurts, and J.A. Leunissen. 2007. Primer3Plus, an enhanced web interface to Primer3. *Nucleic Acids Res.* 35(Web Server issue):W71–W74. http://dx.doi.org/10.1093/nar/gkm306

Vas, A.C., C.A. Andrews, K. Kirkland Matesky, and D.J. Clarke. 2007. In vivo analysis of chromosome condensation in *Saccharomyces cerevisiae. Mol. Biol. Cell*. 18:557–568. http://dx.doi.org/10.1091/mbc.E06-05-0454

Vizeacoumar, F.J., N. van Dyk, F. S Vizeacoumar, V. Cheung, J. Li, Y. Sydorskyy, N. Case, Z. Li, A. Datti, C. Nislow, et al. 2010. Integrating high-throughput genetic interaction mapping and high-content screening to explore yeast spindle morphogenesis. *J. Cell Biol.* 188:69–81. http://dx.doi.org/10.1083/jcb.200909013

Wan, J., D. Subramonian, and X.D. Zhang. 2012. SUMOylation in control of accurate chromosome segregation during mitosis. *Curr. Protein Pept. Sci.* 13:467–481. http://dx.doi.org/10.2174/138920312802430563

Wang, Z., and G. Prelich. 2009. Quality control of a transcriptional regulator by SUMO-targeted degradation. *Mol. Cell. Biol.* 29:1694–1706. http://dx.doi.org/10.1128/MCB.01470-08

Wang, Z., G.M. Jones, and G. Prelich. 2006. Genetic analysis connects SLX5 and SLX8 to the SUMO pathway in *Saccharomyces cerevisiae. Genetics*. 172:1499–1509. http://dx.doi.org/10.1534/genetics.105.052811

Westermann, B., and W. Neupert. 2000. Mitochondria-targeted green fluorescent proteins: convenient tools for the study of organelle biogenesis in *Saccharomyces cerevisiae. Yeast*. 16:1421–1427. http://dx.doi.org/10.1002/1097-0061(200011)16:15<1421::AID-YEA624>3.0.CO;2-U

Wohlschlegel, J.A., E.S. Johnson, S.I. Reed, and J.R. Yates III. 2004. Global analysis of protein sumoylation in *Saccharomyces cerevisiae. J. Biol. Chem.* 279:45662–45668. http://dx.doi.org/10.1074/jbc.M409203200

Wright, R. 2000. Transmission electron microscopy of yeast. *Microsc. Res. Tech.* 51:496–510. http://dx.doi.org/10.1002/1097-0029(20001215)51:6<496::AID-JEMT2>3.0.CO;2-9

Wu, L., and I.D. Hickson. 2006. DNA helicases required for homologous recombination and repair of damaged replication forks. *Annu. Rev. Genet.* 40:279–306. http://dx.doi.org/10.1146/annurev.genet.40.110405.090636

Xiong, L., X.L. Chen, H.R. Silver, N.T. Ahmed, and E.S. Johnson. 2009. Deficient SUMO attachment to Flp recombinase leads to homologous recombination-dependent hyperamplification of the yeast 2 microm circle plasmid. *Mol. Biol. Cell*. 20:1241–1251. http://dx.doi.org/10.1091/mbc.E08-06-0659

Yan, Z., M. Costanzo, L.E. Heisler, J. Paw, F. Kaper, B.J. Andrews, C. Boone, G. Giaever, and C. Nislow. 2008. Yeast Barcoders: a chemogenomic application of a universal donor-strain collection carrying bar-code identifiers. *Nat. Methods*. 5:719–725. http://dx.doi.org/10.1038/nmeth.1231

Yang, S.H., and A.D. Sharrocks. 2004. SUMO promotes HDAC-mediated transcriptional repression. *Mol. Cell*. 13:611–617. http://dx.doi.org/10.1016/S1097-2765(04)00060-7

Yin, Y., A. Seifert, J.S. Chua, J.F. Maure, F. Golebiowski, and R.T. Hay. 2012. SUMO-targeted ubiquitin E3 ligase RNF4 is required for the response of human cells to DNA damage. *Genes Dev.* 26:1196–1208. http://dx.doi.org/10.1101/gad.189274.112

Zhou, W., J.J. Ryan, and H. Zhou. 2004. Global analyses of sumoylated proteins in Saccharomyces cerevisiae. Induction of protein sumoylation by cellular stresses. *J. Biol. Chem.* 279:32262–32268. http://dx.doi.org/10.1074/jbc.M404173200